Journal of Inorganic Biochemistry 196 (2019) 110688

Contents lists available at ScienceDirect

Journal of Inorganic Biochemistry

journal homepage: www.elsevier.com/locate/jinorgbio

# Cobalt(II) complexes with the non-steroidal anti-inflammatory drug diclofenac and nitrogen-donor ligands

Spyros Perontsis[a], Alexandra Dimitriou[a], Panagiota Fotiadou[a], Antonios G. Hatzidimitriou[a], Athanasios N. Papadopoulos[b], George Psomas[a,*]

[a] Laboratory of Inorganic Chemistry, Faculty of Chemistry, Aristotle University of Thessaloniki, GR-54124 Thessaloniki, Greece
[b] Department of Nutrition and Dietetics, Faculty of Food Technology and Nutrition, Alexandrion Technological Educational Institution, Sindos, Thessaloniki, Greece

ARTICLE INFO

*Keywords:*
Diclofenac
Cobalt(II) complexes
Interaction with DNA
Interaction with albumins
Antioxidant activity

ABSTRACT

The interaction of the non-steroidal anti-inflammatory drug sodium diclofenac with $CoCl_2$ in the absence or presence of the nitrogen-donor ligands 2,2′-bipyridine, 1,10-phenanthroline, 2,2′-bipyridylamine, pyridine or imidazole resulted in the formation of six mononuclear Co(II) complexes. The complexes were characterized by diverse physicochemical and spectroscopic techniques and single-crystal X-ray crystallography revealing a monodentate or a bidentate chelating binding mode of the diclofenac ligands. The scavenging activity of the complexes was evaluated *in vitro* against the free radicals of 1,1-diphenyl-2-picrylhydrazyl, 2,2′-azinobis-(3-ethylbenzothiazoline-6-sulfonic acid) (ABTS) and hydroxyl; the complexes present significant scavenging activity of ABTS and hydroxyl radicals. The interaction of the complexes with calf-thymus (CT) DNA and bovine serum albumin (BSA) was also investigated; the complexes can bind tightly to CT DNA *via* intercalation and can bind to BSA tightly and reversibly.

## 1. Introduction

Non-steroidal anti-inflammatory drugs (NSAIDs) are medication agents widely used to relieve pain, reduce inflammation, and lower a high-temperature fever. NSAIDs act by inhibiting the activity of cyclooxygenase enzymes (COX-1 and/or COX-2) non-selectively or COX-2 selectively and, thus, blocking the production of prostaglandins, which are responsible for pain and inflammation [1]. NSAIDs are generally used for the symptomatic relief of conditions such as osteoarthritis, rheumatoid arthritis, low-back pain, headache, migraine, fever, dysmenorrhea, tennis elbow etc. [2]. Furthermore, the interaction between DNA and NSAIDs or the metal-NSAID complexes is of great magnitude because their possible anticancer, antioxidant and anti-inflammatory activity may be explained [3,4].

The most common chemical classes of NSAIDs are phenylalkanoic acids, anthranilic acids, oxicams, salicylate derivatives, sulfonamides and furanones. Sodium diclofenac (Nadicl) (Fig. 1(A)) belongs to the NSAID group of phenylalkanoic acids [5]. It is mainly used to treat pain, inflammatory disorders such as rheumatoid arthritis, polymyositis and osteoarthritis and dysmenorrhea [6]. In the literature, the reported transition metal complexes with diclofenac ligands include those with manganese(II) [7,8], copper(II) [9–11], nickel(II) [12], cobalt(II) [13], tin(II) [14], zinc(II) [15] and cadmium(II) [16].

Cobalt is an essential element for life in trace amounts. There are at least eight cobalt-dependent proteins [17]. However, the main biological role of cobalt concerns its presence in the active center of vitamin B12, which is cofactor in DNA-synthesis and in both fatty acid and amino acid metabolism [18]. Cobalt is involved in the co-enzyme of vitamin B12 used as a supplement of the vitamin [19]. Additionally, cobalt in inorganic form is also a micronutrient for bacteria, algae, and fungi. Since the first reported studies concerning the biological activity of cobalt compounds in 1952 [20], many cobalt complexes of biological interest have been reported with the majority of the structurally characterized ones showing antitumor, antiproliferative [21,22], antimicrobial [23,24], antifungal [25,26], antiviral [27,28] and antioxidant [29] activity.

In most of the reported metal-NSAID complexes, the co-existence of NSAIDs and the N,N′-donor ligands has led to enhanced biologic activity (DNA- and albumin-binding properties and antioxidant activity) in comparison to the corresponding free NSAID [7–14,29–43]. Within this context and as a continuation of our studies concerning metal-NSAID complexes [7–9,12,29–43], we report the interaction of Co(II) with diclofenac in the absence or in the presence of the nitrogen-donor heterocyclic ligands 1,10-phenanthroline (phen), 2,2′-bipyridine (bipy),

* Corresponding author.
*E-mail address:* gepsomas@chem.auth.gr (G. Psomas).

https://doi.org/10.1016/j.jinorgbio.2019.04.002
Received 7 March 2019; Received in revised form 1 April 2019; Accepted 3 April 2019
Available online 05 April 2019
0162-0134/ 

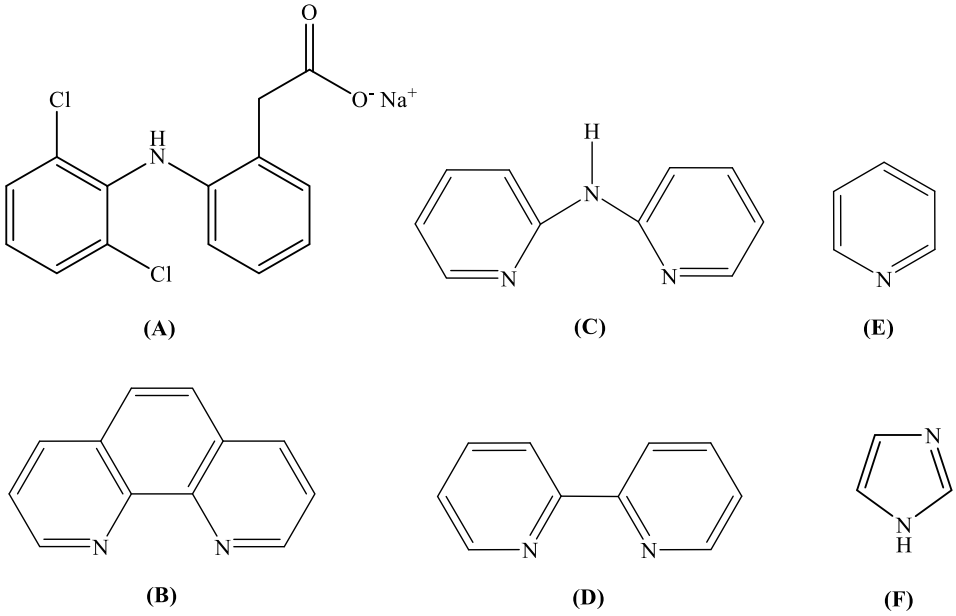


**Fig. 1.** The structural formula of (A) sodium diclofenac (Nadicl), (B) 1,10-phenanthroline (phen), (C) 2,2′-bipyridylamine (bipyam), (D) 2,2′-bipyridine (bipy), (E) pyridine (py) and (F) imidazole (Himi).

2,2′-bipyridylamine (bipyam), pyridine (py) or imidazole (Himi) (Fig. 1(B)–(F)). The resultant complexes $[Co(dicl)_2(MeOH)_4]$ (**1**), $[Co(dicl)_2(phen)]$ (**2**), $[Co(dicl)_2(bipy)]$ (**3**), $[Co(dicl)_2(bipyam)]\cdot 0.5H_2O$ (**4**·$0.5H_2O$), $[Co(dicl)_2(py)_2(H_2O)_2]\cdot py$ (**5**·py) and $[Co(dicl)_2(Himi)_2]\cdot H_2O$ (**6**·$H_2O$) were characterized with physicochemical and spectroscopic techniques. The crystal structures of complexes **2–6** were determined by X-ray crystallography. Furthermore, the antioxidant activity of the complexes was evaluated by determining their ability to scavenge *in vitro* 1,1-diphenyl-picrylhydrazyl (DPPH), 2,2′-azino-bis(3-ethylbenzothiazoline-6-sulfonic acid) ($ABTS^{+}\cdot$) and hydroxyl (·OH) radicals. The potential *in vitro* behavior of the compounds towards biomolecules was investigated through the study of their interaction with calf-thymus (CT) DNA (performed with UV–vis spectroscopy, DNA-viscosity measurements, cyclic voltammetry and competitive studies with ethidium bromide (EB)) and of the binding affinity for bovine serum albumin (BSA) (by fluorescence emission spectroscopy).

## 2. Experimental

### 2.1. Materials - instrumentation - physical measurements

All the chemical reagents, i.e. $CoCl_2\cdot 6H_2O$, sodium diclofenac, phen, bipyam, bipy, py, Himi, KOH, CT DNA, BSA, EB, NaCl, trisodium citrate, DPPH, ABTS, EDTA, butylated hydroxytoluene (BHT), 6-hydroxy-2,5,7,8-tetramethylchromane-2-carboxylic acid (trolox), nordihydroguaiaretic (NDGA), and all solvents were of reagent grade and were used as purchased from commercial sources without any further purification.

DNA stock solution was prepared by the dilution of CT DNA to buffer (containing 15 mM trisodium citrate and 150 mM NaCl at pH 7.0) followed by exhaustive stirring for three days, and kept at 4 °C for no longer than a week. The stock solution of CT DNA gave a ratio of UV absorbance at 260 and 280 nm ($A_{260}/A_{280}$) of 1.87, indicating that the DNA was sufficiently free of protein contamination [44]. The DNA concentration was determined by UV absorbance at 258 nm after 1:20 dilution using $\varepsilon = 6600\ M^{-1}\ cm^{-1}$ [45].

Infrared (IR) spectra (400–4000 $cm^{-1}$) were recorded on a Nicolet FT-IR 6700 spectrometer with samples prepared as KBr disk. UV–visible (UV–vis) spectra were recorded as nujol mulls and in solution at concentrations in the range $10^{-5}$–$10^{-3}$ M on a Hitachi U-2001 dual beam spectrophotometer. C, H and N elemental analysis were performed on a PerkinElmer 240B elemental analyzer. Molar conductivity measurements were carried out with a Crison Basic 30 conductometer. Room temperature magnetic measurements were carried out by the Faraday method using mercury tetrathiocyanatocobaltate(II) as a calibrant. Fluorescence spectra were recorded in solution on a Hitachi F-7000 fluorescence spectrophotometer.

Cyclic voltammetry studies were performed on an Eco chemie Autolab Electrochemical analyzer. Cyclic voltammetry experiments were carried out in a 30-mL three-electrode electrolytic cell. The working electrode was platinum disk, a separate Pt single-sheet electrode was used as the counter electrode and a Ag/AgCl electrode saturated with KCl was used as the reference electrode. The cyclic voltammograms of the complexes were recorded in 0.4 mM 1/2 DMSO/buffer solutions at $v = 100\ mV\ s^{-1}$ where buffer solution was the supporting electrolyte. Oxygen was removed by purging the solutions with pure nitrogen which had been previously saturated with solvent vapors. All electrochemical measurements were performed at 25.0 ± 0.2 °C. Viscosity experiments were carried out using an ALPHA L Fungilab rotational viscometer equipped with an 18 mL LCP spindle and the measurements were performed at 100 rpm.

### 2.2. Synthesis of the complexes

#### 2.2.1. Synthesis of $[Co(dicl)_2(MeOH)_4]$, 1

A methanolic solution (15 mL) containing Nadicl (0.4 mmol, 127 mg) was added dropwise to a methanolic solution (5 mL) of $CoCl_2\cdot 6H_2O$ (0.2 mmol, 48 mg) and the reaction mixture was stirred for 1 h. The reaction solution was filtered and left for slow evaporation. Rose-colored microcrystalline product of $[Co(dicl)_2(MeOH)_4]$, **1**, (85 mg, yield: 55%) was collected after a few days. Anal. Calcd for $[Co(dicl)_2(MeOH)_4]$ ($C_{32}H_{36}Cl_4CoN_2O_8$) (MW = 777.39): C 49.44, H 4.67, 3.60; found C 49.67, H 4.75, N 3.48%. IR (KBr disk), $\nu_{max}/cm^{-1}$: $\nu_{asym}(CO_2)$, 1577(vs (very strong)); $\nu_{sym}(CO_2)$, 1397 (vs); $\Delta\nu(CO_2) = \nu_{asym}(CO_2) - \nu_{sym}(CO_2) = 180\ cm^{-1}$. UV–vis: as nujol mull, λ/nm: 552, 470(shoulder (sh)); in DMSO, λ/nm ($\varepsilon/M^{-1}\ cm^{-1}$): 560 (55), 480(sh) (25), 290 (7900). $\mu_{eff}$ = 3.95 BM at room temperature. The complex is soluble in DMSO and DMF and is non-electrolyte ($\Lambda_M$ = 7 mho·$cm^2$·$mol^{-1}$, in 1 mM DMSO).

*2.2.2. Synthesis of complexes **2–6***

Complexes **2–6** were prepared in a similar way. More specifically, a methanolic solution (15 mL) of Nadicl (0.4 mmol, 127 mg) and the corresponding nitrogen-donor was added to a methanolic solution (5 mL) of $CoCl_2{\cdot}6H_2O$ (0.2 mmol, 48 mg). Gentle stirring for 1 h followed and the filtrate was left for slow evaporation.

*2.2.2.1. [Co(dicl)$_2$(phen)], **2**:*. 1,10-Phenanthroline (0.2 mmol, 36 mg) was used as the nitrogen-donor ligand. Pink-colored crystals of **2** suitable for single-crystal X-ray crystallography were collected after three days. Yield: 125 mg, 75%. Anal. Calcd for [Co(dicl)$_2$(phen)] ($C_{40}H_{28}Cl_4CoN_4O_4$) (MW = 829.43): C 57.92, H 3.40, 6.76; found C 58.07, H 3.53, N 6.49%. IR (KBr disk), $\nu_{max}/cm^{-1}$: $\nu_{asym}(CO_2)$: 1583 (vs); $\nu_{sym}(CO_2)$: 1424 (vs); $\Delta\nu(CO_2) = 159\ cm^{-1}$; $\rho(C\text{-}H)_{phen}$ = 726 (medium (m)). UV–vis: as nujol mull, λ/nm: 520, 480; in DMSO, λ/nm (ε/$M^{-1}\,cm^{-1}$): 515 (50), 470 (40), 292 (13500), 271 (25000). $\mu_{eff}$ = 4.27 BM at room temperature. The complex is soluble in DMF and DMSO ($\Lambda_M$ = 11 mho·cm$^2$·mol$^{-1}$, in 1 mM DMSO).

*2.2.2.2. [Co(dicl)$_2$(bipy)], **3**:*. 2,2′-Bipyridine (0.2 mmol, 31 mg) was used as the nitrogen-donor ligand. Brownish crystals of **3** suitable for single-crystal X-ray crystallography were collected after four days. Yield: 88 mg, 55%. Anal. Calcd for [Co(dicl)$_2$(bipy)] ($C_{38}H_{28}Cl_4CoN_4O_4$) (MW = 805.41): C 56.67, H 3.50, 6.96; found C 56.92, H 3.59, N 7.18%. IR (KBr disk), $\nu_{max}/cm^{-1}$: $\nu_{asym}(CO_2)$: 1575 (vs); $\nu_{sym}(CO_2)$: 1420 (vs); $\Delta\nu(CO_2) = 155\ cm^{-1}$; $\rho(C\text{-}H)_{bipy}$ = 763 (m). UV–vis: as nujol mull, λ/nm: 540, 465(sh); in DMSO, λ/nm (ε/$M^{-1}\,cm^{-1}$): 520 (60), 470(sh) (55), 288(15700). $\mu_{eff}$ = 4.35 BM at room temperature. The complex is soluble in DMSO and DMF ($\Lambda_M$ = 9 mho·cm$^2$·mol$^{-1}$, in 1 mM DMSO).

*2.2.2.3. [Co(dicl)$_2$(bipyam)]·0.5H$_2$O, **4**·*. 0.5$H_2O$: 2,2′-bipyridylamine (0.2 mmol, 34 mg) was as used the nitrogen-donor ligand. Brownish crystalline product suitable for single-crystal X-ray crystallography was deposited after a few days. Yield: 100 mg, 60%. Anal. calcd. for [Co(dicl)$_2$(bipyam)] ($C_{38}H_{29}Cl_4CoN_5O_4$) (MW = 820.43): C 55.63, H 3.56, 8.54; found C 55.42, H 3.71, N 8.69%. IR (KBr disk), $\nu_{max}/cm^{-1}$: $\nu_{asym}(CO_2)$: 1577 (vs); $\nu_{sym}(CO_2)$: 1420 (vs); $\Delta\nu(CO_2) = 157\ cm^{-1}$; $\rho(C\text{-}H)_{bipyam}$ = 770 (m). UV–vis: as nujol mull, λ/nm: 536, 480; in DMSO, λ/nm (ε/$M^{-1}\,cm^{-1}$): 530 (40), 475(sh) (30), 310 (11500), 274 (20500). $\mu_{eff}$ = 4.00 BM at room temperature. The complex is soluble in $CH_3CN$, DMF and DMSO ($\Lambda_M$ = 12 mho·cm$^2$·mol$^{-1}$, in 1 mM DMSO).

*2.2.2.4. [Co(dicl)$_2$(py)$_2$(H$_2$O)$_2$]·py, **5**·*. py: Pyridine (1.5 mL) was used as the nitrogen-donor ligand. Rose-colored single-crystals of **5** suitable for X-ray crystallography were formed after one week. Yield: 90 mg, 55%. Anal. Calcd for [Co(dicl)$_2$(py)$_2$(H$_2$O)$_2$] ($C_{38}H_{34}Cl_4CoN_4O_6$) (MW = 843.46): C 54.11, H 4.06, 6.64; found C 54.01, H 4.27, N 6.78%. IR (KBr disk), $\nu_{max}/cm^{-1}$: $\nu_{asym}(CO_2)$: 1601 (vs); $\nu_{sym}(CO_2)$: 1387 (vs); $\Delta\nu(CO_2) = 214\ cm^{-1}$; $\rho(C\text{-}H)_{py}$ = 700(m). UV–vis: as nujol mull, λ/nm: 603, 480(sh); in DMSO, λ/nm (ε/$M^{-1}\,cm^{-1}$): 530 (30), 476(sh) (25), 289 (7200). $\mu_{eff}$ = 4.28 BM at room temperature. The complex is soluble in chloroform, DMF and DMSO ($\Lambda_M$ = 8 mho·cm$^2$·mol$^{-1}$, in 1 mM DMSO).

*2.2.2.5. [Co(dicl)$_2$(Himi)$_2$]·H$_2$O, **6**·*. $H_2O$: Imidazole (0.4 mmol, 26 mg) was used as the nitrogen-donor ligand. Well-shaped purple crystals suitable for single-crystal X-ray crystallography were obtained after one week. Yield: 85 mg, 52%. Anal. Calcd for [Co(dicl)$_2$(Himi)$_2$] ($C_{34}H_{28}Cl_4CoN_6O_6$) (MW = 785.38): C 51.98, H 3.59, 10.70; found C 51.72, H 3.73, N 10.51%. IR (KBr disk), $\nu_{max}/cm^{-1}$: $\nu_{asym}(CO_2)$: 1574 (vs); $\nu_{sym}(CO_2)$: 1389 (vs); $\Delta\nu(CO_2) = 185\ cm^{-1}$; $\rho(C\text{-}H)_{Himi}$ = 748(m). UV–vis: as nujol mull, λ/nm: 563, 465(sh); in DMSO, λ/nm (ε/$M^{-1}\,cm^{-1}$): 560 (80), 469(sh) (30), 289 (9600). $\mu_{eff}$ = 4.38 BM at room temperature. The complex is soluble in chloroform, DMF and DMSO ($\Lambda_M$ = 13 mho·cm$^2$·mol$^{-1}$, in 1 mM DMSO).

*2.3. X-ray structure determination*

Single-crystals of compounds **2–6** were obtained from reaction mixtures according to the described synthetic procedures. For the structural determination of **2–6**, single-crystals of the respective compounds were mounted on a Bruker Kappa APEX II diffractometer, equipped with a triumph monochromator at ambient temperature. Diffraction measurements were recorded using Mo Kα radiation. Unit cell dimensions were determined by using at least 120 reflections in the range $20 < 2\theta < 40^\circ$. Intensity data were collected using φ and ω scan mode. The frames collected for each crystal were integrated with the Bruker SAINT software package [46] using a narrow-frame algorithm. Data were corrected for absorption using the numerical method (SADABS) based on crystal dimensions [47].

All structures were solved using SUPERFLIP [48] package and refined by full–matrix least-squares method on $F^2$ using the CRYSTALS package version 14.40b [49] All non-disordered non-hydrogen atoms have been refined anisotropically.

All hydrogen atoms were found at their expected positions and refined using soft constraints. By the end of the refinement, they were positioned using riding constraints. The crystal data, details of data collection and structure refinement for all compounds studied are given in Table S1. Illustrations were drawn by CAMERON [50] Further details on the crystallographic studies as well as atomic displacement parameters are given as Supporting Information in the form of cif files.

*2.4. Antioxidant biological assay*

The antioxidant activity of complexes **1–6** was evaluated *via* their ability to scavenge *in vitro* free radicals such as DPPH, hydroxyl and ABTS. All the experiments were carried out at least in triplicate and the standard deviation of absorbance was < 10% of the mean.

*2.4.1. Determination of the reducing activity of the stable radical DPPH*

To an ethanolic solution of DPPH (0.1 mM) an equal volume solution of the compounds (0.1 mM) in ethanol was added. Absolute ethanol was also used as control solution. The absorbance at 517 nm was recorded at room temperature after 20 and 60 min, in order to examine the possible existence of a potential time-dependence of the DPPH radical scavenging activity [51]. The DPPH scavenging activity of the complexes was expressed as the percentage reduction of the absorbance values of the initial DPPH solution (RA %). NDGA and BHT were used as reference compounds.

*2.4.2. Assay of radical cation ABTS scavenging activity*

Initially, a water solution of ABTS was prepared (2 mM). ABTS radical cation ($ABTS^+\cdot$) was produced by the reaction of ABTS stock solution with potassium persulfate (0.17 mM) and the mixture was stored in the dark at room temperature for 12–16 h before its use. The ABTS was oxidized incompletely because the stoichiometric reaction ratio of ABTS and potassium persulfate is 1:0.5. The absorbance became maximal and stable only after > 6 h of reaction although the oxidation of the ABTS started immediately. The radical was stable in this form for > 2 days when allowed to stand in the dark at room temperature. Afterwards, the $ABTS^+\cdot$ solution was diluted in ethanol to an absorbance of 0.70 at 734 nm and 10 μL of diluted compounds or standards (0.1 mM) in DMSO were added. The absorbance was recorded out exactly 1 min after initial mixing [51]. The radical scavenging activity of the complexes was expressed as the percentage inhibition of the absorbance of the initial ABTS solution (ABTS %). Trolox was used as an appropriate standard.

*2.4.3. Competition of the compounds with DMSO for hydroxyl radicals*

According to Nash [52], the hydroxyl radicals which were generated by the $Fe^{3+}$/ascorbic acid system were detected by the determination of formaldehyde produced from the oxidation of DMSO. The

reaction mixture consisted of EDTA (0.1 mM), $FeCl_3$ (167 μM), DMSO (33 mM) in phosphate buffer (50 mM, pH 7.4), ascorbic acid (10 mM) and the tested compounds (0.1 mM). After incubation for 30 min at 37 °C, the reaction was stopped by the addition of $CCl_3COOH$ (17% w/v) and the absorbance at λ = 412 nm was measured. Trolox was the appropriate reference standard that was used. The competition of the compounds with DMSO for ·OH, generated by the $Fe^{3+}$/ascorbic acid system, was expressed as percentage inhibition of formaldehyde production and was used for the evaluation of hydroxyl radical scavenging activity (·OH%).

### 2.5. Binding studies with biomolecules

In order to study the interaction of complexes with DNA and BSA, the compounds were initially dissolved in DMSO (1 mM). Mixing of such solutions with the aqueous buffer solutions DNA or BSA used in the studies never exceeded 5% DMSO (v/v) in the final solution, which was needed due to low aqueous solubility of most compounds. In all experiments, the effect of DMSO on the data has been taken into consideration and the appropriate corrections have been performed.

#### 2.5.1. Binding studies with CT DNA

The interaction of complexes **1–6** with CT DNA was studied by UV–vis spectroscopy, cyclic voltammetry, viscosity measurements and *via* competitive studies with EB by fluorescence emission spectroscopy.

*2.5.1.1. UV–vis spectroscopy:*. UV–vis spectroscopy was used to study the interaction of complexes **1–6** with CT DNA in order to estimate their possible binding mode to CT DNA and calculate the corresponding binding constants ($K_b$). The UV spectra of CT DNA in the presence of each compound were recorded for a constant CT DNA concentration (1.3–1.5 × $10^{-4}$ M) at diverse [compound]/[CT DNA] mixing ratios (*r*). The UV–vis spectra of the compounds were recorded for a standard concentration (20–30 μM) in the absence or presence of increasing concentration of CT DNA for diverse r values and were used to calculate the values of the constant $K_b$ (in $M^{-1}$) by the Wolfe-Shimer equation (eq. S1) [53] and the plots [DNA]/($\varepsilon_A$-$\varepsilon_f$) *versus* [DNA]. Control experiments with DMSO were performed and no changes in the spectra of CT DNA were observed.

*2.5.1.2. DNA-viscosity measurements:*. The viscosity of DNA solution in buffer solution (150 mM NaCl and 15 mM trisodium citrate at pH 7.0) was measured upon increasing amounts of complexes **1–6** (up to the value of $r = 0.35$). All measurements were performed at room temperature and the obtained data are presented as $(\eta/\eta_0)^{1/3}$ *versus r*, where η is the viscosity of DNA in the presence of the compound and $\eta_0$ is the viscosity of DNA alone in buffer solution.

*2.5.1.3. Cyclic voltammetry:*. The interaction of complexes **1–6** with CT DNA was also investigated *via* monitoring the changes observed in the cyclic voltammogram of a 0.40 mM 1:2 DMSO:buffer solution of the complex upon addition of DNA solution at diverse *r* values. The buffer was also used as the supporting electrolyte and the cyclic voltammograms were recorded at $\nu = 100\ mV\ s^{-1}$. The ratio of the DNA-binding constants for the reduced ($K_r$) and oxidized forms ($K_{ox}$) of the complexes ($K_r/K_{ox}$) was calculated according to eq. S2 [54].

*2.5.1.4. EB-competitive studies:*. The competitive studies of complexes **1–6** with EB for the DNA-intercalating sites (by displacing it from its DNA-EB complex) were investigated with fluorescence emission spectroscopy. The CT DNA-EB complex was prepared by pre-treating 20 μM EB and 26 μM CT DNA in buffer (150 mM NaCl and 15 mM trisodium citrate at pH 7.0). The possible replacement of EB by the compounds and thus the intercalating effect was studied by the stepwise addition of a certain amount of a compound's solution into a solution of the DNA-EB conjugate. The effect of the addition of each complex to the DNA-EB solution was obtained by recording the variation of fluorescence emission spectra with excitation wavelength at 540 nm [55]. The complexes do not show any appreciable fluorescence emission bands at room temperature in solution or in the presence of CT DNA or EB under the same experimental conditions ($\lambda_{ex}$ = 540 nm); therefore, the observed quenching of the EB-DNA solution may be attributed to the displacement of EB from its EB-DNA conjugate. The Stern-Volmer constants ($K_{SV}$, in $M^{-1}$) were calculated by the linear Stern-Volmer equation (eq. S3) [56] and the respective plots Io/I *versus* [Q]. Taking $\tau_o$ = 23 ns as the fluorescence lifetime of the EB-DNA conjugate [57], the quenching constants ($k_q$, in $M^{-1}\ s^{-1}$) of the complexes were calculated according to eq. S4.

#### 2.5.2. Albumin binding studies

The BSA-binding study was performed by tryptophan fluorescence quenching experiments using BSA (3 μM) in buffer (containing 15 mM trisodium citrate and 150 mM NaCl at pH 7.0). The fluorescence emission spectra were recorded with an excitation wavelength of 295 nm. The quenching of the emission intensity of tryptophan residues of BSA at 343 nm was monitored using complexes **1–6** as quenchers with gradually increasing concentration. Except to this, the fluorescence emission spectra of the complexes were also recorded with $\lambda_{ex}$ = 295 nm and an emission band appeared at $\lambda_{max}$ = 365 nm which is typical for metal-diclofenac compounds [7–9,12]; thus, the BSA fluorescence emission spectra were corrected by subtracting the spectra of the compounds. The influence of the inner-filter effect on the measurements was evaluated by eq. S5 [58]. The Stern-Volmer and Scatchard equations (eqs. S3, S4 and S6) [59] and graphs were used in order to calculate the Stern-Volmer constant $K_{SV}$ (in $M^{-1}$), the quenching constant $k_q$ (in $M^{-1}\ s^{-1}$), the SA-binding constant K (in $M^{-1}$) and the number of binding sites per albumin n.

## 3. Results and discussion

### 3.1. Synthesis and characterization of the complexes

The preparation of complexes **1–6** in high yield was achieved *via* the aerobic reaction of a methanolic solution of Nadicl with $CoCl_2{\cdot}6H_2O$ in a 1:2 $Co^{2+}$:$dicl^{-1}$ ratio for **1** (reaction 1), while the presence of the corresponding nitrogen-donor ligand (L) yielded complexes **2–6**. A 1:2:1 $Co^{2+}$:$dicl^{-1}$:L ratio afforded complexes **2–4**, e.g. phen for **2** (reaction 2); for complexes **5** and **6**, a 1:2:2 $Co^{2+}$:$dicl^{-1}$:L ratio was used, e.g. Himi for **6** (reaction 3):

$$CoCl_2{\cdot}6H_2O + 2\ Nadicl + 4\ CH_3OH \rightarrow [Co(dicl)_2(CH_3OH)_4] + 2\ NaCl + 6\ H_2O \quad (1)$$

$$CoCl_2{\cdot}6H_2O + 2\ Nadicl + phen \rightarrow [Co(dicl)_2(phen)] + 2\ NaCl + 6\ H_2O \quad (2)$$

$$CoCl_2{\cdot}6H_2O + 2\ Nadicl + 2\ Himi \rightarrow [Co(dicl)_2(Himi)_2] + 2\ NaCl + 6\ H_2O \quad (3)$$

The compounds were characterized by IR and UV–vis spectroscopy, room-temperature magnetic measurements and by single-crystal X-ray crystallography (for **2–6**). The complexes are stable in the air, soluble in DMSO and DMF and insoluble in most organic solvents and $H_2O$. The complexes do not dissociate in DMSO ($\Lambda_M$ = 7–13 mho·$cm^2$·$mol^{-1}$ in $10^{-3}$ M DMSO solution), and we may conclude that they keep their integrity.

The magnetic measurements of the complexes were performed at room temperature according to Faraday method and values of $\mu_{eff}$ were found in the range 3.95–4.38 BM. These values are higher than the expected spin-only value ($\mu_{eff}$ = 3.87 BM) showing spin-orbit coupling due to $t_{2g}^5e_g^2$ electron configuration, albeit lower than other reported octahedral mononuclear high-spin Co(II) complexes [17]. These values

may support a distorted octahedral geometry around Co(II) ion (with S = 3/2) [17].

### 3.2. Spectroscopic study of the complexes

IR spectroscopy may be used to investigate the existence of the ligands and their coordination mode in the complexes. In the IR spectrum of Nadicl, two intense bands located at 1575(s) and 1399(s) $cm^{-1}$ may be attributed to the characteristic stretching vibrations of the carboxylic group of diclofenac, i.e. the antisymmetric, $\nu_{asym}(CO_2)$, and the symmetric, $\nu_{sym}(CO_2)$, respectively. In the IR spectra of the complexes, these bands have shifted to the regions 1574–1601 and 1387–1424 $cm^{-1}$, respectively, showing the binding of diclofenac ligands to Co(II). In order to further clarify the coordination mode of the carboxylato group of diclofenac ligands, the parameter $\Delta\nu(CO_2)$ ($=\nu_{asym}(CO_2) - \nu_{sym}(CO_2)$) [60] was determined for complexes **1–6**. For **1**, **5** and **6**, the parameter $\Delta\nu(CO_2)$ has a value of 180, 214 $cm^{-1}$ and 185 $cm^{-1}$, respectively, which is higher than the $\Delta\nu(CO_2)$ value in Nadicl (176 $cm^{-1}$) and is indicative of monodentate binding of the carboxylato group of diclofenac [60,61]. For complexes **2–4**, the $\Delta\nu(CO_2)$ value lies in the range 155–159 $cm^{-1}$, which is indicative of a bidentate chelating mode of binding [61]. The conclusions concerning the coordination mode of the carboxylato group of diclofenac ligands are in good agreement with the crystal structures of the complexes discussed in Section 3.3.

The existence of the corresponding nitrogen-donor ligands and their coordination to cobalt(II) were verified *via* the characteristic bands attributed to the out-of-plane ρ(C-H) vibrations which were found at 726(m) $cm^{-1}$ for $\rho(C\text{-}H)_{phen}$ in complex **2**, 763(m) $cm^{-1}$ for $\rho(C\text{-}H)_{bipy}$ in **3**, 770(m) $cm^{-1}$ for $\rho(C\text{-}H)_{bipyam}$ in **4**, 700(m) $cm^{-1}$ for $\rho(C\text{-}H)_{py}$ in **5**, and 748(m) $cm^{-1}$ for $\rho(C\text{-}H)_{Himi}$ in **6** [60].

The UV–vis spectra of the complexes were recorded as nujol mull and in DMSO solution and are similar suggesting that the complexes retain their structure in solution. In the visible region, for **1–5**, two low-intensity bands are observed and may be assigned to d-d transitions. More specifically, the band located in the region 515–560 nm may be attributed to a $^4T_{1g}(F) \rightarrow {}^4A_{2g}$ transition, and the band at 469–480 nm may be due to a $^4T_{1g}(F) \rightarrow {}^4T_{1g}(P)$ transition; the locations of these bands are typical for distorted octahedral high-spin $Co^{2+}$ complexes [17]. The visible region of the spectrum of **6** is dominated by the highest energy $^4A_2 \rightarrow {}^4T_1(P)$ transition band observed at 560 nm, which is a typical one for tetrahedral Co(II) complexes [17]. Additionally, an absorption band assigned to an intraligand transition exists at 288–310 nm.

Bearing in mind that complexes **1–6** are non-electrolytes in DMSO solution and they have the same UV–vis spectral pattern in nujol and in DMSO solution as well as in the presence of the buffer solution used in the biological experiments (and in combination with the non-electrolytic nature of the complexes), we may conclude that the compounds keep their integrity in solution.

### 3.3. Structure of the complexes

For complexes **2–6**, single-crystals suitable for X-ray crystallography have been obtained. Therefore, their crystal structures were determined by X-ray crystallography. Complex **1** was obtained as microcrystalline product and its structure was proposed on the basis of all experimental data and in comparison with the literature.

#### 3.3.1. Crystal structures of complexes *2–4*

The crystal structures of the complexes **2–4** are similar and they will be discussed together. The complexes are mononuclear with the diclofenac ligands being coordinated in an asymmetrical bidentate chelating mode to cobalt atom *via* the two carboxylato oxygen atoms. A diagram of the structures of complexes **2–4** is shown in Figs. 2 and 3 and selected bond distances and angles are listed in Tables 1 and 2.

The six-coordinate cobalt atom is surrounded by two diclofenac ligands and one bidentate phen for **2**, bipy for **3** or bipyam ligand for **4** showing a distorted octahedral geometry. Thus, two nitrogen and four oxygen atoms giving a $CoN_2O_4$ chromophore occupy the six vertices of the octahedron. The structures of the complexes are stabilized by the development of intraligand and, especially for complex **4**, intermolecular hydrogen bonds. More specifically, the amino group of diclofenac ligand is involved in intraligand H-bonding with the coordinated carboxylato group (Table S2). In addition, the structure of **4** is further stabilized by intermolecular hydrogen bonds between H atoms of solvate water molecules H(52) and H(384) and carboxylato oxygen atoms O(2)′ or O(2)″, respectively, of adjacent molecules.

A thorough search of the Cambridge Crystallographic Data Centre (CCDC) database regarding the mononuclear Co(II) complexes with carboxylato ligands and the N,N′-donors phen, bipyam and bipy has revealed the existence of at least five examples with phen ligands [62–64], less structures with bipyam [32,33,65], and only one with a bipy ligand [66], bearing similar arrangement of the atoms around Co (II) with general formula $[Co(RCOO\text{-}O,O')_2(N,N'\text{-donor})]$. It is interesting to note that the search of Co(II) complexes with monodentate carboxylato ligands (either in $[Co(RCOO\text{-}O)(RCOO\text{-}O,O')(N,N'\text{-donor})(O\text{-donor})]$ or in $[Co(RCOO\text{-}O)_2(N,N'\text{-donor})(O\text{-donor})_2]$ complexes, where the co-existence of O-donor ligand(s) was necessary for the stabilization of the distorted geometry) did not reveal any structures with bipyam as co-ligand, while this number increased significantly in the case of co-ligand bipy [29,33,67–69]. For phen, all three different arrangements around Co(II) seem to have equal number of examples [70–75].

#### 3.3.2. Crystal structure of complex *5*

The crystal structure of the mononuclear complex **5** is given in Fig. 4 and selected bond distances and angles are cited in Table 3.

In this complex, the diclofenac ligands are monodentately bound to cobalt(II) ion *via* a carboxylate oxygen. The structure of the complex is centrosymmetric, the cobalt(II) ion is sitting on a center of symmetry and is coordinated to two diclofenac, two pyridine and two aqua ligands showing an octahedral geometry. The basal plane of the octahedron is formed by the carboxylate oxygen atoms O(1) and the aqua oxygen atoms O(3) while the pyridine nitrogen atoms N(1) are found in the axial positions at 2.154(3) Å. In the equatorial plane of the octahedron, the bond distances $Co\text{-}O_{carb}$ (2.084(2) Å) and $Co\text{-}O_{aqua}$ (2.098(2) Å) are similar. The uncoordinated carboxylate oxygen atoms are lying out of the $CoO_4$ plane at distances Co(1)···O(2) = 3.283 Å. A research in CCDC has revealed few examples of crystal structures of mononuclear Co(II) complexes with carboxylate, pyridine and O-donor (e.g. $H_2O$) ligands in a similar arrangement around the metal [31,76–78].

The structure of complex **5** is further stabilized by the presence of intermolecular hydrogen bonds. Intermolecular hydrogen-bonds are formed between the aqua hydrogen atoms H(32) and H(31) and the uncoordinated oxygen atom O(2) of diclofenac ligand and N(3) of the pyridine solvate molecule as well as between H(32) and O(2′) of an adjacent molecule (Table S2).

#### 3.3.3. Crystal structure of complex *6*

The molecular structure of complex **6** is shown in Fig. 5 and selected bond distances and angles are presented in Table 4.

The cobalt atom is four-coordinate and is surrounded by two monodentate diclofenac and two imidazole ligands showing a distorted tetrahedral geometry. The tetrahedrality for a four-coordinated cobalt complex can be determined from the angle which is formed by two planes each enclosing the cobalt and two adjacent atoms (for strictly square planar complexes with $D_{4h}$ symmetry, the tetrahedrality is 0° while for tetrahedral complexes with $D_{2d}$ symmetry, the tetrahedrality equals 90°) [79]. For complex **6**, the tetrahedrality determined by the dihedral angle of planes O(1), Co(1), N(1) and O(3), Co(1), N(3) has the

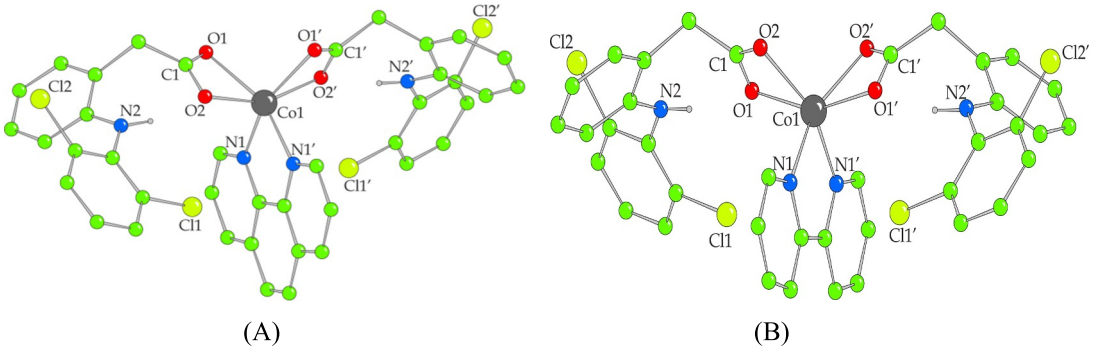


**Fig. 2.** Crystal structures of (A) $[Co(dicl)_2(phen)]$, **2** and (B) $[Co(dicl)_2(bipy)]$, **3**. Hydrogen atoms are emitted for clarity.

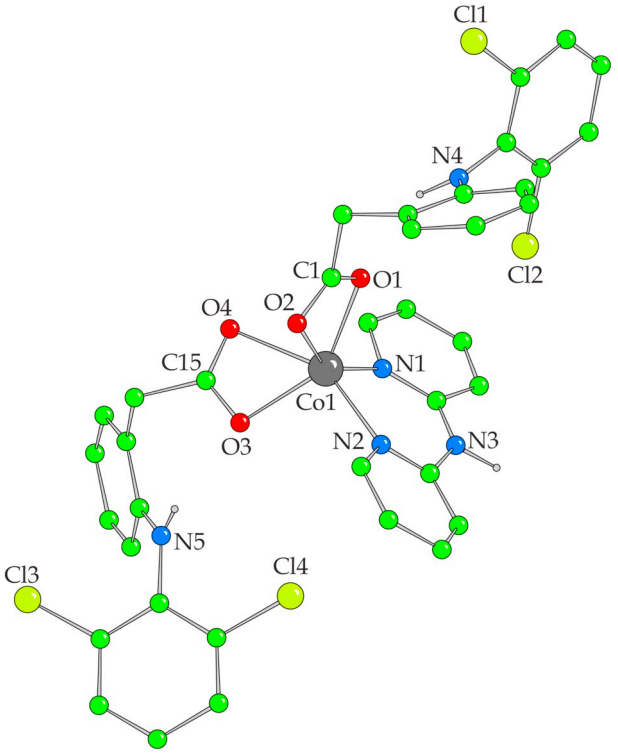


**Fig. 3.** A drawing of the crystal structure of **4** and only the heteroatom labeling.

value of 75.64°; therefore, we may support a tetrahedral geometry for the chromophore $CoO_2N_2$. The tetrahedral geometry around Co(1) was further verified by the values of tetrahedral index $\tau_4$ or $\tau'_4$ as introduced by Yang ($\tau_4 = (360° - (\alpha + \beta))/(360° - 2 \times 109.5°)$, where α and β are the largest angles around the metal [80] and Okuniewski ($\tau'_4 = ((\beta - \alpha)/(360° - 109.5°)) + ((180° - \beta)/(180° - 109.5°))$ where $\beta > \alpha$ are the largest angles of the coordination sphere) [81], respectively. The values of these parameters are $\tau_4 = 0.84$ and $\tau'_4 = 0.81$ and are close to 1 supporting a tetrahedral geometry around Co(1).

The distances around Co(1) are within the expected range and the Co-$N_{Himi}$ distances [Co(1)-N(1) = 2.026(3) Å, Co(1)-N(3) = 2.019(3) Å] are slightly longer than the Co-$O_{carboxylate}$ distances [Co(1)-O(1) = 2.004(2) Å, Co(1)-O(3) = 2.004(2) Å]. The distances of Co(1) with the non-coordinated carboxylate atoms O(2) and O(4) are rather long (Co(1)…O(2) = 2.498 Å and Co(1)…O(4) = 3.080 Å) to suggest a bonding distance. The structure of complex **6** is stabilized by the development of intraligand and intermolecular hydrogen-bonds. Intraligand H-bonds are formed between the NH-group and the carboxylate oxygen atoms O(2) and O(3) of diclofenac ligands (Table S2). The hydrogen atoms of the solvate water molecule participate in weak intermolecular interactions with the uncoordinated O(4) of the diclofenac ligand and coordinated O(1)′ of the diclofenac ligand of an adjacent molecule contributing to further stabilization of the complex (Table S2).

A thorough search of the CCDC concerning the mononuclear Co(II) complexes with carboxylato ligands and imidazole derivatives has revealed a few relevant structures where Co(II) may be in either four- or

**Table 1**
Selected bond distances (Å) and bond angles (°) for complexes **2** and **3**.

| Bond | Complex 2 | Complex 3 |
|---|---|---|
| | Distance (Å) | Distance (Å) |
| Co(1)-O(1) | 2.180 (2) | 2.105(2) |
| Co(1)-O(2) | 2.073 (2) | 2.139(2) |
| Co(1)-N(1) | 2.092 (3) | 2.073(3) |
| O(1)-C(1) | 1.245 (3) | 1.251(4) |
| O(2)-C(1) | 1.257 (4) | 1.245(4) |

| Bonds | Complex 2 | Complex 3 |
|---|---|---|
| | Angle (°) | Angle (°) |
| O(1)-Co(1)-O(2) | 60.84 (8) | 60.82 (9) |
| O(1)-Co(1)-O(1)′ | 97.73 (14) | 155.47 (14) |
| O(1)-Co(1)-O(2)′ | 102.05 (10) | 102.21 (9) |
| O(1)-Co(1)-N(1) | 96.50 (10) | 103.66 (11) |
| O(1)-Co(1)-N(1)′ | 154.02 (8) | 95.27 (10) |
| O(2)-Co(1)-O(2)′ | 155.56 (15) | 99.01 (15) |
| O(2)-Co(1)-N(1) | 103.86 (10) | 95.95 (12) |
| O(2)-Co(1)-N(1)′ | 94.94 (9) | 153.98 (9) |
| N(1)-Co(1)-N(1)′ | 79.44 (14) | 78.97 (19) |

**Table 2**
Selected bond distances (Å) and angles (°) for complex **4**.

| Bond | Distance (Å) | Bond | Distance (Å) |
|---|---|---|---|
| Co(1)-O(1) | 2.056 (3) | Co(1)-N(2) | 2.066 (4) |
| Co(1)-O(2) | 2.331 (3) | O(1)-C(1) | 1.253 (6) |
| Co(1)-O(3) | 2.063 (3) | O(2)-C(1) | 1.231 (6) |
| Co(1)-O(4) | 2.356 (4) | O(3)-C(15) | 1.231 (6) |
| Co(1)-N(1) | 2.057 (4) | O(4)-C(15) | 1.219 (6) |

| Bonds | Angle (°) | Bonds | Angle (°) |
|---|---|---|---|
| O(1)-Co(1)-O(2) | 59.13 (12) | O(2)-Co(1)-O(3) | 93.13 (14) |
| O(1)-Co(1)-O(3) | 141.81 (13) | O(2)-Co(1)-O(4) | 92.76 (14) |
| O(1)-Co(1)-O(4) | 95.58 (13) | O(2)-Co(1)-N(1) | 150.50 (12) |
| O(1)-Co(1)-N(1) | 91.87 (13) | O(2)-Co(1)-N(2) | 95.64 (14) |
| O(1)-Co(1)-N(2) | 112.24 (13) | O(4)-Co(1)-N(1) | 95.58 (14) |
| O(3)-Co(1)-O(4) | 57.23 (12) | O(4)-Co(1)-N(2) | 151.34 (13) |
| O(3)-Co(1)-N(1) | 115.11 (13) | N(1)-Co(1)-N(2) | 90.45 (15) |
| O(3)-Co(1)-N(2) | 94.91 (13) | | |

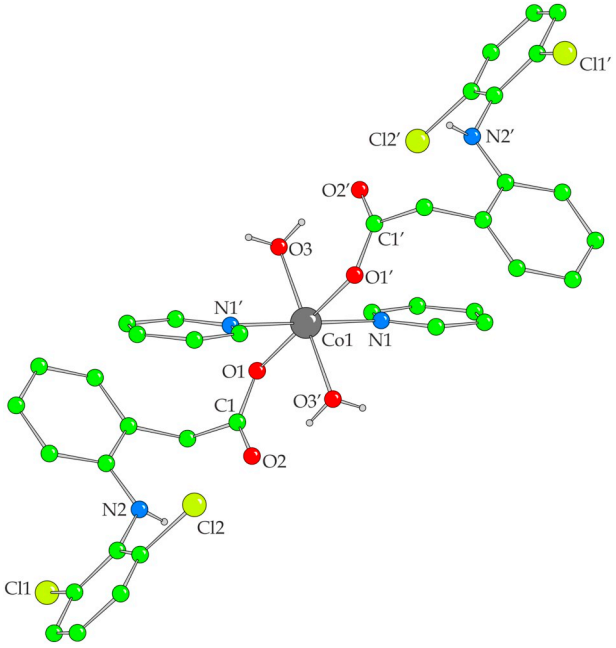


**Fig. 4.** The molecular structure of **5** with only the heteroatom labeling.

**Table 3**
Selected bond distances (Å) and angles (°) for **5**.

| Bond | Distance (Å) |
|---|---|
| Co(1)-N(1) | 2.154 (3) |
| Co(1)-O(1) | 2.084 (2) |
| Co(1)-O(3) | 2.098 (2) |
| C(1)-O(1) | 1.264 (4) |
| C(1)-O(2) | 1.233 (4) |

| Bonds | Angle (°) |
|---|---|
| O(1)-Co(1)-N(1) | 91.88 (11) |
| O(1)-Co(1)-N(1)′ | 88.12 (11) |
| O(1)-Co(1)-O(3) | 87.44 (10) |
| O(1)-Co(1)-O(3)′ | 92.56 (10) |
| O(3)-Co(1)-N(1) | 85.22 (11) |
| O(3)-Co(1)-N(1)′ | 94.78 (11) |

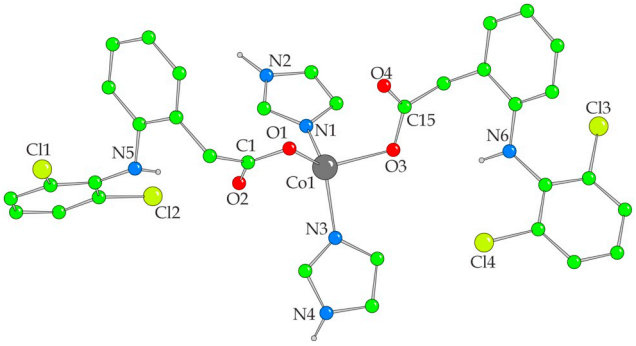


**Fig. 5.** Crystal structure of $[Co(dicl)_2(Himi)_2]\cdot H_2O$, **6**. Hydrogen atoms are omitted for clarity.

six-coordinate environment. The four-coordinate complexes have the formula $[Co(RCOO\text{-}O)_2(Himi)_2]$ with monodentately coordinated carboxylato ligands [82–86] and similar arrangements of the atoms around Co as in complex **6**. The six-coordinate complexes may bear the formula $[Co(RCOO\text{-}O,O')_2(Himi)_2]$, i.e. bidentate chelating coordination mode of the carboxylato ligands [85,75], or $[Co(RCOO\text{-}O)_2(Himi)_2(H_2O)_2]$,

**Table 4**
Selected bond distances (Å) and angles (°) for complex **6**.

| Bond | Distance (Å) | Bond | Distance (Å) |
|---|---|---|---|
| Co(1)-O(1) | 2.004 (2) | O(1)-C(1) | 1.255 (4) |
| Co(1)-O(3) | 2.004 (2) | O(2)-C(1) | 1.281 (4) |
| Co(1)-N(1) | 2.026 (3) | O(3)-C(15) | 1.310 (4) |
| Co(1)-N(3) | 2.019 (3) | O(4)-C(15) | 1.221 (4) |

| Bonds | Angle (°) | Bonds | Angle (°) |
|---|---|---|---|
| O(1)-Co(1)-N(1) | 110.90 (10) | O(3)-Co(1)-N(1) | 94.56 (10) |
| O(1)-Co(1)-N(3) | 111.69 (10) | O(3)-Co(1)-N(3) | 95.65 (10) |
| O(1)-Co(1)-O(3) | 116.90 (9) | N(1)-Co(1)-N(3) | 125.09 (11) |

i.e. monodentate coordination of the carboxylato ligands and the co-existence of two aqua ligands [87–89].

### 3.3.4. *Proposed structure for complex **1***

The efforts to isolate single-crystals of compound **1** suitable for X-ray crystallography did not yield any crystalline product. Therefore, the characterization of this complex was based on the data collected by magnetic measurements, IR and UV–vis spectroscopy and in comparison with the reported structures of Co(II) complexes with the NSAIDs mefenamic acid (=Hmef), diflunisal (=Hdifl) and niflumic acid (=Hnif). Based on the magnetic data ($\mu_{eff}$ = 3.95 BM), a mononuclear high-spin Co(II) complex (S = 3/2) is suggested, in good agreement with the UV–vis spectrum of the complexes which contained bands typical for a Co(II) complex with a distorted octahedral geometry. The IR spectroscopic study revealed that diclofenac ligands are coordinated to cobalt ion monodentately ($\Delta\nu(CO_2) = 180\ cm^{-1}$). In conclusion, complex **1** bears a $CoO_6$ coordination environment consisting of two carboxylato oxygen atoms of diclofenac ligands and four oxygen atoms from the coordinated methanol ligands. This suggested arrangement of the NSAIDs and methanol ligands is similar to that of complexes $[Co(mef)_2(MeOH)_4]\cdot 2MeOH$ [29], $[Co(difl)_2(MeOH)_4]$ and $[Co(nif)_2(MeOH)_4]$ [32], which have been previously reported by our lab.

### 3.4. *Antioxidant activity of the complexes*

Free radicals are species playing an important role in the inflammatory process. Antioxidants may reduce and/or prevent the damage from free radical reactions because of their ability to donate electrons which may further neutralize the radical without forming another one. NSAIDs are related with the inhibition of free radical production acting as radical scavengers [90]. Thus, the potential anti-inflammatory and possible anticancer activity of sodium diclofenac and its complexes **1–6** may be evaluated initially by investigating their ability to scavenge free radicals such as DPPH, ABTS and hydroxyl radicals.

DPPH scavengers are considered antiageing, anticancer and anti-inflammatory agents and so they may offer protection against rheumatoid arthritis and inflammation. Compounds capable to scavenge hydroxyl radicals (·OH) may serve as protectors from the reactive oxygen species by activation of the prostaglandins. The scavenging of the cationic ABTS radicals ($ABTS^{+}\cdot$) is considered as an indicator of the total antioxidant activity [51]. Additionally, the resultant antioxidant activity of the compounds has been compared to common antioxidant agents NDGA, BHT and trolox which are used as the reference standard compounds of the present studies (Table 5).

The DPPH-scavenging activity of the complexes, except complex **5**, is not time-dependent as concluded by measurements performed after 20 and 60 min (Table 5). For complex **5**, the activity against DPPH presents a notable increase during time. On average, complexes **1–6** exhibit low-to-moderate ability to scavenge DPPH radicals, when compared to reference compounds NDGA and BHT, and are more

**Table 5**
% DPPH scavenging ability (RA%), % superoxide radical scavenging activity (ABTS%) and competition % with DMSO for hydroxyl radical (·OH%), for complexes **1–6**.

| Compound | RA% (20 min) | RA% (60 min) | ABTS% | ·OH % |
|---|---|---|---|---|
| Nadicl [7] | 18.26 ± 0.60 | 17.43 ± 0.23 | 76.35 ± 0.75 | 75.46 ± 0.44 |
| $[Co(dicl)_2(MeOH)_4]$, **1** | 22.38 ± 0.61 | 23.42 ± 0.72 | 81.23 ± 0.52 | 91.42 ± 0.94 |
| $[Co(dicl)_2(phen)]$, **2** | 21.58 ± 0.86 | 18.73 ± 0.37 | 87.68 ± 0.91 | 89.95 ± 1.24 |
| $[Co(dicl)_2(bipy)]$, **3** | 20.38 ± 0.46 | 20.49 ± 0.28 | 84.32 ± 0.57 | 92.51 ± 0.64 |
| $[Co(dicl)_2(bipyam)]$, **4** | 26.17 ± 0.48 | 26.86 ± 0.75 | 91.16 ± 0.59 | 96.33 ± 1.82 |
| $[Co(dicl)_2(py)_2(H_2O)_2]$, **5** | 19.96 ± 0.72 | 25.43 ± 0.83 | 86.12 ± 1.43 | 90.04 ± 0.97 |
| $[Co(dicl)_2(Himi)_2]$, **6** | 24.19 ± 0.68 | 22.41 ± 0.73 | 88.56 ± 1.24 | 96.11 ± 1.06 |
| NDGA | 81.02 ± 0.18 | 82.60 ± 0.17 | Not tested | Not tested |
| BHT | 31.30 ± 0.10 | 60.00 ± 0.38 | Not tested | Not tested |
| Trolox | Not tested | Not tested | 91.80 ± 0.17 | 82.80 ± 0.13 |

effective DPPH-scavengers than free Nadicl. The scavenging ability of the compounds against the cationic ABTS radical ($ABTS^{+}\cdot$) is much better than free Nadicl and quite high compared to the reference compound trolox (Table 5). Furthermore, it is worth mentioning that the ability of **1–6** to scavenge hydroxyl radicals is higher than not only free Nadicl but also than the reference compound trolox. Summarizing the data of the present study, complexes **1–6** present higher scavenging ability than free Nadicl showing thus that binding of the NSAID to Co (II) results in enhanced activity. In addition, complex **4** is the most potent radical scavenger of all the free radicals examined.

In addition, the Co-diclofenac complexes are better DPPH-scavengers than some of their Co-NSAIDs analogues [32], while their hydroxyl and ABTS scavenging ability is of the same magnitude with all reported Co-NSAIDs compounds [29,31,32]. Also, the Mn-diclofenac analogues [7] may present a lower ability to scavenge ABTS free radicals than **1–6** while the activity against the other free radicals was found in the same range. The antioxidant activity of the complexes may be considered to be selective, especially against hydroxyl and ABTS radicals since they show low to moderate activity against DPPH and high activity against hydroxyl and ABTS radicals.

### 3.5. Interaction of complexes with CT DNA

In many cases, the potential bioactivity of NSAIDs and their metal complexes has been connected with the ability to interact with DNA [4], which could be considered a potential biological target. In general, the interaction of metal complexes with DNA depends on the stability of the complexes and the nature of the ligands and may take place *via* the development of covalent (a bond is formed between metal and a DNA-base displacing a labile ligand of the complex) or noncovalent interactions (intercalation, groove-binding or electrostatic interactions resulting from π-π stacking, hydrophobic or Coulomb forces, respectively) [91]. We have already reported the DNA-binding behavior of a series of metal-NSAID complexes [29–43], including also those containing diclofenac ligands [7–9,12]. As a continuation of our previous research, the interaction of complexes **1–6** with CT DNA was studied by UV–vis spectroscopy, cyclic voltammetry, viscosity measurements and *via* competitive studies with EB by fluorescence emission spectroscopy.

#### 3.5.1. DNA-binding study with UV–vis spectroscopy

UV–vis spectroscopy is a technique used to provide information about the mode of interaction of metal complexes with CT DNA and the strength of this interaction. The UV spectra were recorded for a constant CT DNA concentration in different [compound]/[DNA] mixing ratios (*r*) and are shown representatively for **1** in Fig. 6(A). The slight decrease of the intensity at $\lambda_{max}$ = 258 nm is accompanied by a red-shift of the $\lambda_{max}$, suggesting the interaction with CT DNA which may result in the direct formation of a new complex with double-helical CT DNA [92].

In UV–vis spectra of **1–6**, an intraligand band (band I) appears at 288–292 nm while in the case of **2** and **4** an additional band (band II) is present at 271–275 nm similar to previously reported diclofenac complexes [7]. The absorbance and the position of these bands may differ upon addition of a CT DNA solution. More specifically, in the UV–vis spectra of **2**, both bands (band I at 292 nm and band II at 271 nm) exhibit, in the presence of increasing amounts of CT DNA a slight hypochromism (Fig. 6(B)). In the UV–vis spectra of **5**, the band at 289 nm exhibits a slight hyperchromism (Fig. 6(C)). Similar is the behavior of the other complexes in the presence of DNA (Table 6). A safe outcome regarding the interaction mode of the complexes with DNA cannot be taken because of the low percentages of the observed hyper- or hypochromism [92,93]. Thus, further studies regarding the DNA-interaction of the complexes were carried out in order to better clarify the exact mode, i.e. cyclic voltammetry and viscosity measurements.

The DNA-binding constants of **1–6** ($K_b$) were calculated by the plots [DNA]/($\varepsilon_A$-$\varepsilon_f$) *versus* [DNA] (Fig. S1) with the Wolfe-Shimer equation (eq. S1) [53]. The $K_b$ values of **1–6** (Table 6) are significantly higher than that of free Nadicl suggesting stronger binding to DNA. Especially, the $K_b$ value of complex **1** ($=1.65(\pm 0.02) \times 10^7\,M^{-1}$) is significantly high and is the highest value among all reported Co-NSAIDs [29–33] and metal-diclofenac complexes [7–9,11,12]. The $K_b$ values of all complexes are higher than that of the classical intercalator EB ($K_b = 1.23(\pm 0.07) \times 10^5\,M^{-1}$) as reported in literature [94].

#### 3.5.2. DNA-binding study with cyclic voltammetry

Cyclic voltammetry is an electrochemical technique that provides useful information regarding the mechanism of interaction of metal compounds with DNA. Any changes observed at the cyclic voltammograms of the complexes in the presence of DNA may be indicative of an interaction between the compounds and DNA [54]. The cyclic voltammograms of complexes **1–6** were recorded in a 1/2 DMSO/buffer solution (0.33 mM) in the absence and presence of CT DNA (representatively shown for complex **6** in Fig. 7). The observed decrease of the current intensity may suggest the existence of equilibrium between free and DNA-bound complex as evidence of the complex-DNA interaction. The cathodic $E_{pc}$ and anodic $E_{pa}$ potentials of the redox couple Co(II)/Co(I) for **1–6** as well as their shifts upon addition of CT DNA are given in Table 7. When CT DNA is added in the solution of the complexes, both the cathodic and the anodic potentials exhibit a positive shift ($\Delta E_{pc/a} = (+8) - (+45)$ mV), suggesting intercalation as the most possible mode of interaction between the complexes and CT DNA bases [30–33].

Additionally, the corresponding equilibrium constants for the redox process were evaluated by determining the ratio of the DNA-binding constants for the reduced form ($K_r$) and oxidized forms ($K_{ox}$) of the complexes ($K_r/K_{ox}$) with eq. S2 [54]. The ratio of equilibrium binding constants, $K_r/K_{ox}$ is calculated in the range 1.15–1.99 (Table 7) which indicates the stronger binding of DNA with the reduced form of complexes **1–6** over its oxidized form [95].

#### 3.5.3. DNA-binding study with viscosity measurements

The DNA-viscosity is sensitive to DNA-length changes, since the

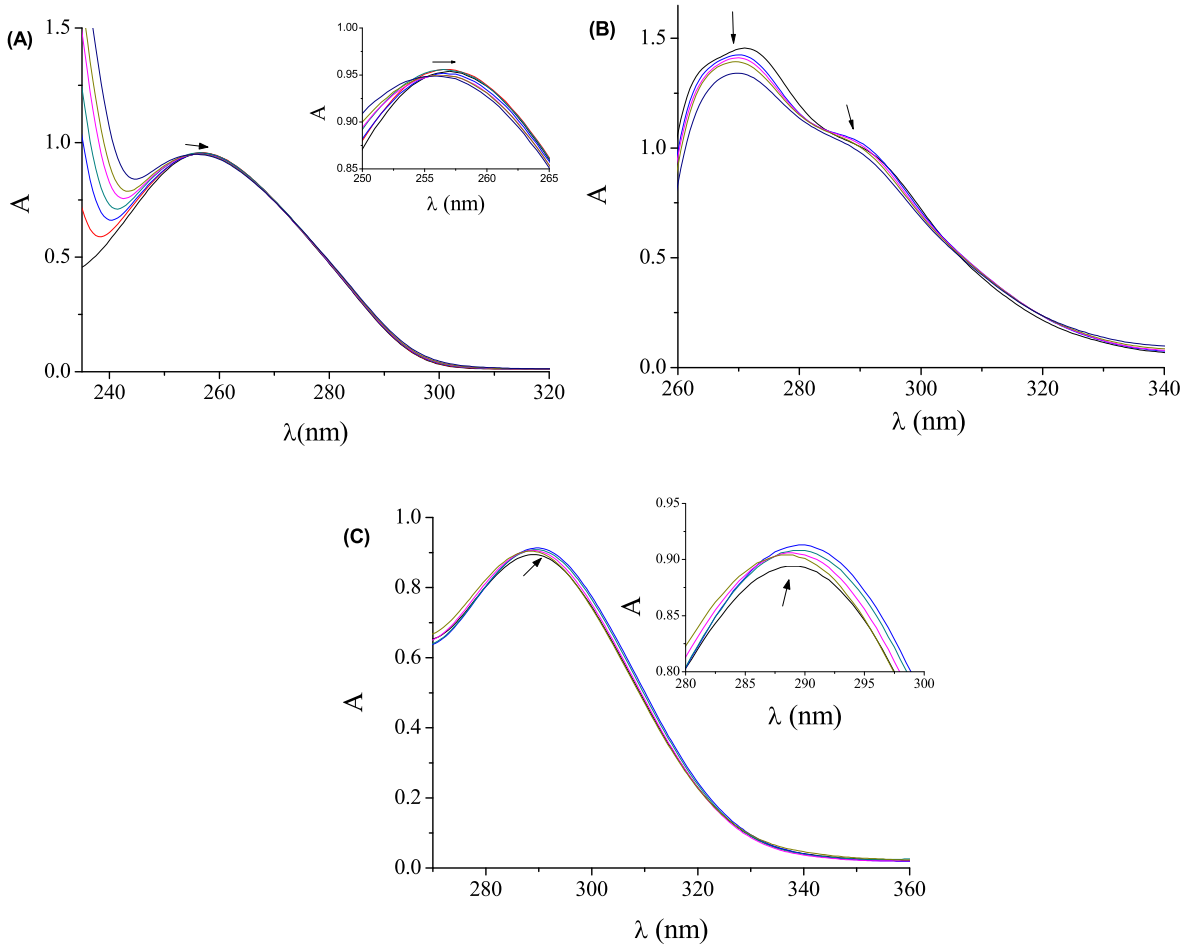


**Fig. 6.** (A) UV spectra of CT DNA ($1.45 \times 10^{-4}$ M) in buffer solution (150 mM NaCl and 15 mM trisodium citrate at pH 7.0) in the absence or presence of [Co(dicl)$_2$(MeOH)$_4$], **1**. The arrow shows the changes upon increasing amounts of the complex. (B)–(C) UV–vis spectra of DMSO solution of complex (B) **2** (30 μM) and (C) **5** (30 μM), in the presence of increasing amounts of CT DNA. The arrows show the changes upon addition of increasing amounts of CT DNA.

**Table 6**
UV-vis spectral features of the interaction of Nadicl and complexes **1–6** with. CT DNA. UV-band (λ in nm) (percentage of the observed hyper-/hypo-chromism ($\Delta A/A_0$, %), blue-/red-shift of the $\lambda_{max}$ ($\Delta\lambda$, nm)) and DNA-binding constants ($K_b$).

| Compound | λ (nm) ($\Delta A/A_0$ (%)[a], $\Delta\lambda$ (nm)[b]) | $K_b$ ($M^{-1}$) |
|---|---|---|
| Nadicl [9] | 295 (−7.5, 0) | 3.16 ( ± 0.14) × $10^4$ |
| [Co(dicl)$_2$(MeOH)$_4$], **1** | 290 (+3, 0) | 1.65 ( ± 0.02) × $10^7$ |
| [Co(dicl)$_2$(phen)], **2** | 271 (−7, 0), 292 (−3, +1) | 2.33 ( ± 1.04) × $10^5$ |
| [Co(dicl)$_2$(bipy)], **3** | 288 (+4, 0) | 9.41 ( ± 0.16) × $10^6$ |
| [Co(dicl)$_2$(bipyam)], **4** | 275 (−3, +1), 288 (+2, 0) | 1.86 ( ± 1.03) × $10^5$ |
| [Co(dicl)$_2$(py)$_2$(H$_2$O)$_2$], **5** | 289 (+2, +1) | 6.41 ( ± 2.04) × $10^5$ |
| [Co(dicl)$_2$(Himi)$_2$], **6** | 289 (+3, 0) | 3.85 ( ± 1.49) × $10^5$ |

[a] "+" denotes hyperchromism, "−" denotes hypochromism.
[b] "+" denotes red-shift, "−" denotes blue-shift.

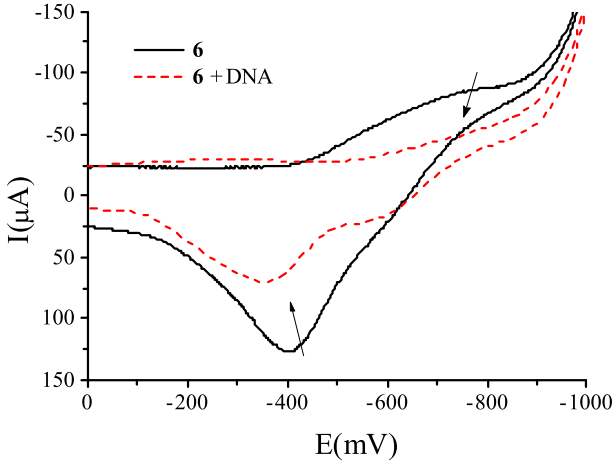


**Fig. 7.** Cyclic voltammogram of 0.4 mM 1/2 DMSO/buffer (containing 150 mM NaCl and 15 mM trisodium citrate at pH = 7.0) solution of complex **6** in the absence or presence of CT DNA. Scan rate = 100 mV $s^{-1}$. Supporting electrolyte = buffer solution.

DNA-viscosity and DNA-length are related *via* the equation $L/L_0 = (\eta/\eta_0)^{1/3}$, with $\eta/\eta_0$ denoting the relative solution viscosity and $L/L_0$ the DNA-length [96]. Consequently, monitoring the viscosity changes of a DNA solution in the presence of increasing amounts of complexes **1–6** may provide significant information in regard to the DNA-binding mode of the compounds. Within this context, the viscosity measurements were carried out on a CT DNA solution (0.1 mM) in the presence of increasing amounts of **1–6** (up to the value of $r = 0.35$). The experiments showed a significant increase of the DNA-viscosity in the presence of increasing amounts of the complexes (Fig. 8). This result may be explained *via* the insertion of the complexes between the DNA-base pairs resulting in an increase in the separation distance of DNA-base pairs at intercalation sites and, thus, an increase in the DNA-length. Such conclusions are in agreement with cyclic voltammetry data, shedding light to the UV-spectroscopic data regarding the DNA-binding

**Table 7**
Cathodic and anodic potentials (in mV) for the redox couples of **1–6** in DMSO/buffer solution in the absence or presence of CT DNA. Ratio of equilibrium binding constants, $K_r/K_{ox}$.

| Compound | $E_{pc(f)}$ [a] | $E_{pc(b)}$ [b] | $\Delta E_{pc}$ [c] | $E_{pa(f)}$ [a] | $E_{pa(b)}$ [b] | $\Delta E_{pa}$ [c] | $K_r/K_{ox}$ |
|---|---|---|---|---|---|---|---|
| $[Co(dicl)_2(MeOH)_4]$, **1** | −789 | −750 | +39 | −438 | −421 | +17 | 1.61 |
| $[Co(dicl)_2(phen)]$, **2** | −753 | −716 | +37 | −389 | −377 | +12 | 1.51 |
| $[Co(dicl)_2(bipy)]$, **3** | −783 | −760 | +23 | −399 | −374 | +25 | 1.50 |
| $[Co(dicl)_2(bipyam)]$, **4** | −770 | −762 | +8 | −370 | −362 | +8 | 1.15 |
| $[Co(dicl)_2(py)_2(H_2O)_2]$, **5** | −755 | −728 | +27 | −415 | −389 | +26 | 1.57 |
| $[Co(dicl)_2(Himi)_2]$, **6** | −785 | −740 | +45 | −406 | −370 | +36 | 1.99 |

[a] $E_{pc/a}$ in DMSO/buffer in the absence of CT DNA ($E_{pc/a(f)}$).
[b] $E_{pc/a}$ in DMSO/buffer in the presence of CT DNA ($E_{pc/a(b)}$).
[c] $\Delta E_{pc/a} = E_{pc/a(b)} - E_{pc/a(f)}$.

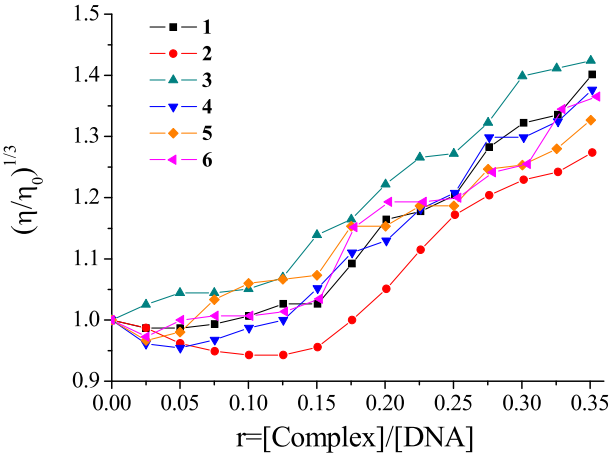


**Fig. 8.** Relative viscosity $(\eta/\eta_0)^{1/3}$ of CT DNA (0.1 mM) in buffer solution (150 mM NaCl and 15 mM trisodium citrate at pH 7.0) in the presence of complexes **1–6** at increasing amounts ($r$ = [complex]/[DNA]).

mode of complexes **1–6**.

### 3.5.4. Competitive study with ethidium bromide

EB is a typical marker of intercalation to DNA which occurs *via* the insertion of its planar phenanthridine ring in-between the CT DNA-base pairs. The result of this intercalation is the appearance of an intense fluorescence emission band at 592 nm, when the EB-DNA solution is excited at 540 nm. The presence of an intercalating compound in this solution will probably induce a quenching of this emission band which may stem from the competition between the intercalating compound and EB. Fluorescence emission spectroscopy was employed to investigate the ability of the complexes to displace the typical DNA-intercalator EB from its EB-DNA complex [55,97].

Upon addition of **1–6** at increasing $r$ values (up to the value of $r$ = 0.14, representatively shown for complex **4** in Fig. 9(A)) into a pretreated solution of EB-DNA, a remarkable quenching of the emission band of the DNA-EB system at 592 nm appeared (up to ~70% of the initial EB-DNA fluorescence) (Fig. 9(B), Table 8). Since the complexes do not present any appreciable fluorescence emission band under the same experimental conditions at room temperature in solution either alone or in the presence of CT DNA or EB, the observed quenching of DNA-EB fluorescence may be ascribed to the displacement of EB by complexes **1–6**, in accordance to the linear Stern-Volmer equation (Eq. S3) and the corresponding Stern-Volmer plots (Fig. S2, $R$ = 0.99), and may reveal indirectly the interaction with CT DNA by intercalation [55,97].

The values of the $K_{sv}$ of the complexes (Table 8) are high enough to validate their ability to bind tightly to DNA. The values of $K_{sv}$ of the complexes are of the same magnitude with that of free Nadicl and complex **6** bears the highest $K_{sv}$ value (=5.62 ( ± 0.18) × $10^5$ $M^{-1}$) among the compounds. The $K_{sv}$ values are lower than those of the Mn-diclofenac [7] and Co-tolfenamato [33] analogues while they are in the same range with the Ni-diclofenac [12] and Co-diclofenac [9] analogues and a series of reported corresponding Co-NSAID complexes [29–32] The quenching constants of the compounds in regard to their competition with EB were calculated with eq. S4, where the fluorescence lifetime of EB-DNA system has the value $\tau_o$ = 23 ns [56]. The $k_q$ constants (Table 8) are significantly higher than $10^{10}$ $M^{-1}$ $s^{-1}$ and we may suggest that the quenching of the EB-DNA fluorescence from the complexes takes place *via* a static mechanism leading to the formation of a new conjugate between DNA and complexes **1–6** [55].

### 3.6. Interaction of the complexes with BSA

The investigation of the possible interaction of bioactive compounds (such as complexes **1–6**) with albumin is essential because this protein is involved in the transportation of ions, compounds and drugs through the bloodstream. Binding to albumin may lead to loss or enhancement of the biological properties of the potential drug, or provide paths for drug transportation [98]. BSA is the most studied albumin due to its homology to human serum albumin. The two tryptophan residues of BSA located at positions 134 and 212 are responsible for the intense fluorescence emission band at 343 nm, when the BSA solution is excited at 295 nm. Therefore, the changes observed in the fluorescence emission spectra of BSA were monitored upon addition of complexes **1–6** to BSA, upon excitation at 295 nm, in order to explore the binding of the complexes with BSA.

The fluorescence quenching of the BSA solution in the presence of the complexes was significant-to-high (quenching up to 97.9% of the initial fluorescence for complex **4**, Fig. 10). This quenching may be attributed to changes in tryptophan environment of BSA which are induced by changes in the albumin's secondary structure because of the interaction of the complexes with BSA; therefore the binding of the complexes to BSA may be indirectly concluded [99].

The Stern-Volmer and Scatchard plots (Figs. S3–S4) and the corresponding equations (eqs. S3, S4 and S6) were used to calculate the constants relevant to the interaction of the complexes with BSA. From these equations and taking $\tau_o = 10^{-8}$ s as fluorescence lifetime of tryptophan [59], the BSA-quenching constant ($k_q$) and the BSA-binding constant (K) were calculated and they are listed in Table 9. The values of $k_q$ are of the order $10^{13}$–$10^{14}$ $M^{-1}$ $s^{-1}$ and are significantly higher than the values found for other quenchers interacting with biopolymers ($2 \times 10^{10}$ $M^{-1}$ $s^{-1}$); therefore, a static quenching mechanism may be suggested [99], verifying the interaction of complexes with BSA. The $k_q$ values of **1–6** are higher than that of free Nadicl and are within the range found for a series of complexes previously reported [7–9,31–33]. Additionally, it is worth mentioning that the $k_q$ value (=2.27( ± 0.10) × $10^{14}$ $M^{-1}$ $s^{-1}$) of complex **4** is the highest observed for all the metal-diclofenac complexes reported [7–12].

The values of K for the complexes are relatively high (of the order $10^5$–$10^6$ $M^{-1}$) and of the same magnitude with a series of metal-NSAID

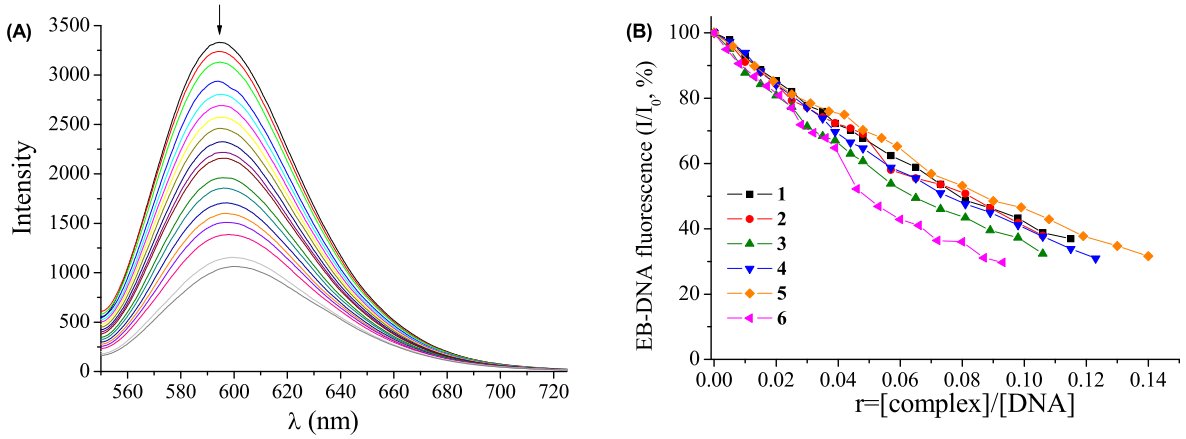


**Fig. 9.** (A) Fluorescence emission spectra ($\lambda_{exc}$ = 540 nm) for EB–DNA ([EB] = 20 μM, [DNA] = 26 μM) in buffer solution in the absence and presence of increasing amounts of complex **4** (up to the value of $r$ = 0.12). The arrow shows the changes of intensity upon increasing amounts of **4**. (B) Plot of EB-DNA relative fluorescence intensity (%I/$I_o$) at $\lambda_{em}$ = 592 nm *versus* r (r = [complex]/[DNA]) in buffer solution (150 mM NaCl and 15 mM trisodium citrate at pH 7.0) in the presence of complexes **1–6** (fluorescence up to 37% of the initial EB-DNA fluorescence for **1**, 37.9% for **2**, 32.3% for **3**, 31% for **4**, 31.7% for **5** and 29.7% for **6**).

complexes previously reported [7–12,29–43]. In conclusion, the K values of **1–6** may be considered high enough to suggest their binding to BSA and their subsequent transportation through the bloodstream. These values are also lower than the association constant of one of the strongest known non-covalent interactions, i.e. avidin with diverse ligands with $K \approx 10^{15}\,M^{-1}$. Thus, the complexes are not too tightly bound to the BSA suggesting indirectly their reversible binding to BSA so that they may get released upon arrival at the targets [100].

## 4. Conclusions

Six novel cobalt(II) complexes with the NSAID diclofenac as ligand and a series of N′-donors 2,2′-bipyridylamine, 1,10-phenanthroline, 2,2′-bipyridine, pyridine or imidazole as co-ligands have been successfully prepared and thoroughly characterized. The crystal structures of five out of six complexes (i.e. complexes **2–6**, namely [Co(dicl)$_2$(phen)] (**2**), [Co(dicl)$_2$(bipy)] (**3**), [Co(dicl)$_2$(bipyam)]·0.5$H_2O$ (**4**·0.5$H_2O$), [Co(dicl)$_2$(py)$_2$($H_2O$)$_2$]·py (**5**·py) and [Co(dicl)$_2$(Himi)$_2$]·$H_2O$ (**6**·$H_2O$)) were determined by single-crystal X-ray crystallography. In these complexes, the diclofenac ligands are bound to cobalt(II) ion in a monodentate and/or a bidentate fashion.

The biological activity of the resultant complexes was evaluated *in vitro* concerning their ability to scavenge free radicals (i.e. DPPH, ABTS and hydroxyl) as well as their ability to bind to CT DNA and their affinity to BSA. Considering the radical scavenging activity, complexes **1–6** are better scavengers than free Nadicl for all the free radicals examined. The DPPH-scavenging ability of the complexes is moderate and stable with the exception of complex **5** which shows increased activity during time. The complexes are significantly active against hydroxyl and ABTS radicals; especially, the hydroxyl scavenging of the complexes is higher than that of the reference compound trolox.

The complexes interact with CT DNA *via* an intercalative mode and

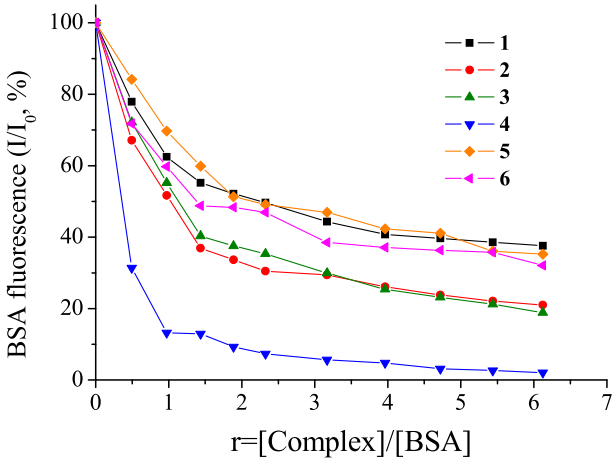


**Fig. 10.** Plot of relative fluorescence intensity of the BSA emission band at $\lambda_{em}$ = 343 nm (I/Io, %) *versus* $r$ ($r$ = [complex]/[BSA]) for complexes **1–6** (up to 37.5% of the initial BSA fluorescence for **1**, 21.9% for **2**, 19.9% for **3**, 2.1% for **4**, 35.2% for **5**, and 32.1% for **6**) in buffer solution (150 mM NaCl and 15 mM trisodium citrate at pH 7.0).

their binding to CT DNA is tight, as evaluated *via* the $K_b$ constants calculated. All complexes bind to CT DNA more tightly than free Nadicl with complex **1** showing the highest DNA-binding constant among the Co-NSAID complexes reported sofar.

The complexes may bind to BSA tightly and reversibly. Therefore, they may be transferred by albumin to potential biological targets where they may be released.

The existing results concerning the bioactivity of Co-diclofenac complexes **1–6** are promising for further biological studies and

**Table 8**
Percentage of EB-DNA fluorescence quenching (ΔI/Io, %), Stern-Volmer ($K_{SV}$) and quenching constants ($k_q$) of complexes **1–6** from the EB-displacement studies.

| Compound | ΔI/$I_0$ (%) | $K_{sv}$ ($M^{-1}$) | $k_q$ ($M^{-1}\,s^{-1}$) |
|---|---|---|---|
| Nadicl [9] | 65.0 | 2.47 ( ± 0.06) × $10^5$ | 1.07 ( ± 0.03) × $10^{13}$ |
| [Co(dicl)$_2$(MeOH)$_4$], **1** | 63.0 | 2.38 ( ± 0.08) × $10^5$ | 1.03 ( ± 0.03) × $10^{13}$ |
| [Co(dicl)$_2$(phen)], **2** | 62.1 | 2.29 ( ± 0.06) × $10^5$ | 9.97 ( ± 0.27) × $10^{12}$ |
| [Co(dicl)$_2$(bipy)], **3** | 67.7 | 3.06 ( ± 0.08) × $10^5$ | 1.33 ( ± 0.03) × $10^{13}$ |
| [Co(dicl)$_2$(bipyam)], **4** | 69.0 | 2.56 ( ± 0.07) × $10^5$ | 1.11 ( ± 0.03) × $10^{13}$ |
| [Co(dicl)$_2$(py)$_2$($H_2O$)$_2$], **5** | 68.3 | 2.61 ( ± 0.07) × $10^5$ | 1.14 ( ± 0.03) × $10^{13}$ |
| [Co(dicl)$_2$(Himi)$_2$], **6** | 70.3 | 5.62 ( ± 0.18) × $10^5$ | 2.44 ( ± 0.08) × $10^{13}$ |

**Table 9**
The BSA-quenching ($k_q$) and BSA-binding (K) constants for complexes **1–6**.

| Compound | $k_q$ ($M^{-1} s^{-1}$) | K ($M^{-1}$) |
|---|---|---|
| Nadicl [9] | 8.11 ( ± 0.34) × $10^{12}$ | 3.55 ( ± 0.03) × $10^5$ |
| $[Co(dicl)_2(MeOH)_4]$, **1** | 1.21 ( ± 0.09) × $10^{13}$ | 3.71 ( ± 0.16) × $10^5$ |
| $[Co(dicl)_2(phen)]$, **2** | 2.15 ( ± 0.09) × $10^{13}$ | 3.93 ( ± 0.03) × $10^5$ |
| $[Co(dicl)_2(bipy)]$, **3** | 2.27 ( ± 0.06) × $10^{13}$ | 2.84 ( ± 0.09) × $10^5$ |
| $[Co(dicl)_2(bipyam)]$, **4** | 2.27 ( ± 0.10) × $10^{14}$ | 1.41 ( ± 0.02) × $10^6$ |
| $[Co(dicl)_2(py)_2(H_2O)_2]$, **5** | 1.02 ( ± 0.05) × $10^{13}$ | 2.14 ( ± 0.09) × $10^5$ |
| $[Co(dicl)_2(Himi)_2]$, **6** | 1.62 ( ± 0.09) × $10^{13}$ | 3.92 ( ± 0.17) × $10^5$ |

potential applications.

## Abbreviations

| | |
|---|---|
| ABTS | 2,2′-azino-bis(3-ethylbenzothiazoline-6-sulfonic acid) |
| BHT | butylated hydroxytoluene |
| bipy | 2,2′-bipyridine |
| bipyam | 2,2′-bipyridylamine |
| BSA | bovine serum albumin |
| CCDC | Cambridge Crystallographic Data Centre |
| $dicl^{-1}$ | anion of diclofenac |
| DPPH | 1,1-diphenyl-picrylhydrazyl |
| EB | ethidium bromide |
| $E_{pa}$ | anodic potential |
| $E_{pc}$ | cathodic potential |
| Hdifl | diflunisal |
| Himi | imidazole |
| Hmef | mefenamic acid |
| Hnif | niflumic acid |
| K | SA-binding constant |
| $K_b$ | DNA-binding constant |
| $k_q$ | quenching constant |
| $K_{SV}$ | Stern-Volmer constant |
| m | medium |
| Nadicl | sodium diclofenac |
| NDGA | nordihydroguaiaretic |
| NSAID | non-steroidal anti-inflammatory drug |
| phen | 1,10-phenanthroline |
| py | pyridine |
| *r* | [compound]/[DNA] mixing ratio or [compound]/[BSA] mixing ratio |
| RA% | % DPPH-scavenging ability |
| s | strong |
| sh | shoulder |
| trolox | 6-hydroxy-2,5,7,8-tetramethylchromane-2-carboxylic acid |
| vs | very strong |
| $\Delta E_{pc/a}$ | $E_{pc/a(b)} - E_{pc/a(f)}$ |
| $\Delta\nu(CO_2)$ | $\nu_{asym}(CO_2) - \nu_{sym}(CO_2)$ |
| $\lambda_{ex}$ | excitation wavelength |

## Acknowledgement

The author SP acknowledges the financial support via a scholarship from the General Secretariat for Research and Technology (GSRT) and Hellenic Foundation for Research and Innovation (HFRI), Greek Ministry of Education, Research and Religion.

## Appendix A. Supplementary data

CCDC 1899212-1899216 contain the supplementary crystallographic data for this paper. These data can be obtained free of charge via www.ccdc.cam.ac.uk/conts/retrieving.html (or from the Cambridge Crystallographic Data Centre, 12 Union Road, Cambridge CB21EZ, UK; fax: (+44) 1223-336-033; or deposit@ccde.cam.ac.uk). Supplementary data associated with this article can be found, in the online version, at https://doi.org/10.1016/j.jinorgbio.2019.04.002.

## References

[1] H.B. Fung, H.L. Kirschenbaum, Clin. Ther. 21 (7) (1999) 1131–1157.
[2] C.P. Duffy, C.J. Elliott, R.A. O'Connor, M.M. Heenan, S. Coyle, I.M. Cleary, K. Kavanagh, S. Verhaegen, C.M. O'Loughlin, R. Nic Amhlaoibh, M. Clynes, Eur. J. Cancer 34 (1998) 1250–1259.
[3] T. Zhang, T. Otevrel, Z.Q. Gao, Z.P. Gao, S.M. Ehrlich, J.Z. Fields, B.M. Boman, Cancer Res. 61 (2001) 8664–8667.
[4] S. Roy, R. Banerjee, M. Sarkar, J. Inorg. Biochem. 100 (2006) 1320–1331.
[5] J.E. Weder, C.T. Dillon, T.W. Hambley, B.J. Kennedy, P.A. Lay, J.R. Biffin, H.L. Regtop, N.M. Davies, Coord. Chem. Rev. 232 (2002) 95–126.
[6] J. Sharma, A.K. Singla, S. Dhawan, Int. J. Pharm. 260 (2003) 217–227.
[7] M. Zampakou, A.G. Hatzidimitriou, A.N. Papadopoulos, G. Psomas, J. Coord. Chem. 68 (2015) 4355–4372.
[8] M. Zampakou, V. Tangoulis, C.P. Raptopoulou, V. Psycharis, A.N. Papadopoulos, G. Psomas, Eur. J. Inorg. Chem. (2015) 2285–2294.
[9] F. Dimiza, F. Perdih, V. Tangoulis, I. Turel, D.P. Kessissoglou, G. Psomas, J. Inorg. Biochem. 105 (2011) 476–489.
[10] D. Kovala-Demertzi, A. Theodorou, M.A. Demertzis, C.P. Raptopoulou, A. Terzis, J. Inorg. Biochem. 65 (1997) 151–157.
[11] S. Kumar, R.P. Sharma, P. Venugopalan, V. Ferretti, S. Perontsis, G. Psomas, J. Inorg. Biochem. 187 (2018) 97–108.
[12] M. Kyropoulou, C.P. Raptopoulou, V. Psycharis, G. Psomas, Polyhedron 61 (2013) 126–136.
[13] S. Caglar, I.E. Aydemir, M. Cankaya, M. Kuzucu, E. Temel, O. Buyukgungor, J. Coord. Chem. 67 (2014) 969–985.
[14] N. Kourkoumelis, M.A. Demertzis, D. Kovala-Demertzi, A. Koutsodimou, A. Moukarika, Spectrochim. Acta A 60 (2004) 2253–2259.
[15] H.A. Ali, B. Jabali, Polyhedron 107 (2016) 97–106.
[16] D. Kovala-Demertzi, D. Mentzafos, A. Terzis, Polyhedron 12 (1993) 1361–1370.
[17] P.V. Bernhardt, G.A. Lawrance, J.A. McCleverty, T.J. Meyer (Eds.), Comprehensive Coordination Chemistry II, vol. 6, Elsevier, 2003, pp. 1–45.
[18] K. Yamada, A. Sigel, H. Sigel, R.K.O. Sigel (Eds.), Metal Ions in Life Sciences: Interrelations between Essential Metal Ions and Human Diseases, vol. 13, Springer, 2013, pp. 295–320.
[19] P.J. Sadler, Adv. Inorg. Chem. 36 (1991) 1–48.
[20] M.D. Hall, T.W. Failes, N. Yamamoto, T.W. Hambley, Dalton Trans. (2007) 3983–3990.
[21] H. Lopez-Sandoval, M.E. Londono-Lemos, R. Garza-Velasco, I. Poblano-Melendez, P. Granada-Macias, I. Gracia-Mora, N. Barba-Behrens, J. Inorg. Biochem. 102 (2008) 1267–1276.
[22] I. Ott, A. Abraham, P. Schumacher, H. Shorafa, G. Gastl, R. Gust, B. Kircher, J. Inorg. Biochem. 100 (2006) 1903–1906.
[23] D.U. Miodragovic, G.A. Bogdanovic, Z.M. Miodragovic, M.D. Radulovic, S.B. Novakovic, G.N. Kaludjerovic, H. Kozlowski, J. Inorg. Biochem. 100 (2006) 1568–1574.
[24] K. Nomiya, A. Yoshizawa, K. Tsukagoshi, N.C. Kasuga, S. Hirakawa, J. Watanabe, J. Inorg. Biochem. 98 (2004) 46–60.
[25] J. Lv, T. Liu, S. Cai, X. Wang, L. Liu, Y. Wang, J. Inorg. Biochem. 100 (2006) 1888–1896.
[26] Z. Weiqun, Y. Wen, X. Liqun, C. Xianchen, J. Inorg. Biochem. 99 (2005) 1314–1319.
[27] A. Bottcher, T. Takeuchi, K.I. Hardcastle, T.J. Meade, H.B. Gray, Inorg. Chem. 36 (1997) 2498–2504.
[28] T. Takeuchi, A. Bottcher, C.M. Quezada, T.J. Meade, H.B. Gray, Bioorg. Med. Chem. 7 (1999) 815–819.
[29] F. Dimiza, A.N. Papadopoulos, V. Tangoulis, V. Psycharis, C.P. Raptopoulou, D.P. Kessissoglou, G. Psomas, Dalton Trans. 39 (2010) 4517–4528.
[30] G. Psomas, D.P. Kessissoglou, Dalton Trans. 42 (2013) 6252–6276.
[31] F. Dimiza, A.N. Papadopoulos, V. Tangoulis, V. Psycharis, C.P. Raptopoulou, D.P. Kessissoglou, G. Psomas, J. Inorg. Biochem. 107 (2012) 54–64.
[32] S. Tsiliou, L.-A. Kefala, A.G. Hatzidimitriou, D.P. Kessissoglou, F. Perdih, A.N. Papadopoulos, I. Turel, G. Psomas, J. Inorg. Biochem. 160 (2016) 125–139.
[33] S. Tsiliou, L.-A. Kefala, F. Perdih, I. Turel, D.P. Kessissoglou, G. Psomas, Eur. J. Med. Chem. 48 (2012) 132–142.
[34] F. Dimiza, C.P. Raptopoulou, V. Psycharis, A.N. Papadopoulos, G. Psomas, New J. Chem. 42 (2018) 16666–16681.
[35] A. Tadic, J. Poljarevic, M. Krstić, M. Kajzerberger, S. Arandelovic, S. Radulovic, C. Kakoulidou, A.N. Papadopoulos, G. Psomas, S. Grgurić-Sipka, New J. Chem. 42 (2018) 3001–3019.
[36] R.P. Sharma, S. Kumar, P. Venugopalan, V. Ferretti, A. Tarushi, G. Psomas, M. Witwicki, RSC Adv. 6 (2016) 88546–88558.
[37] A. Tarushi, C.P. Raptopoulou, V. Psycharis, D.P. Kessissoglou, A.N. Papadopoulos, G. Psomas, J. Inorg. Biochem. 176 (2017) 100–112.
[38] A. Tarushi, C. Kakoulidou, C.P. Raptopoulou, V. Psycharis, D.P. Kessissoglou, I. Zoi, A.N. Papadopoulos, G. Psomas, J. Inorg. Biochem. 170 (2017) 85–97.
[39] A. Tarushi, P. Kastanias, C.P. Raptopoulou, V. Psycharis, D.P. Kessissoglou, A.N. Papadopoulos, G. Psomas, J. Inorg. Biochem. 163 (2016) 332–345.
[40] A. Tarushi, S. Perontsis, A.G. Hatzidimitriou, A.N. Papadopoulos, D.P. Kessissoglou, G. Psomas, J. Inorg. Biochem. 149 (2015) 68–79.
[41] X. Totta, C. Papadopoulou, A.G. Hatzidimitriou, A. Papadopoulos, G. Psomas, J. Inorg. Biochem. 45 (2015) 79–93.

[42] S. Perontsis, A.G. Hatzidimitriou, A.N. Papadopoulos, G. Psomas, J. Inorg. Biochem. 162 (2016) 9–21.
[43] S. Perontsis, A.G. Hatzidimitriou, O.-A. Begou, A.N. Papadopoulos, G. Psomas, J. Inorg. Biochem. 162 (2016) 22–30.
[44] J. Marmur, J. Mol. Biol. 3 (1961) 208–211.
[45] M.F. Reichmann, S.A. Rice, C.A. Thomas, P. Doty, J. Am. Chem. Soc. 76 (1954) 3047–3053.
[46] Bruker Analytical X-ray Systems, Inc., Apex2, Version 2 User Manual, M86-E01078, Madison, WI, (2006).
[47] Siemens Industrial Automation, Inc, SADABS: Area-Detector Absorption Correction, Madison, WI (1996).
[48] P.W. Betteridge, J.R. Carruthers, R.I. Cooper, K. Prout, D.J. Watkin, J. Appl. Crystallogr. 36 (2003) 1487.
[49] L. Palatinus, G.J. Chapuis, Appl. Cryst. 40 (2007) 786–790.
[50] D.J. Watkin, C.K. Prout, L.J. Pearce, Cameron, Chemical Crystallography Laboratory, Oxford, UK, 1996.
[51] C. Kontogiorgis, D. Hadjipavlou-Litina, J. Enz. Inhib. Med. Chem. 18 (2003) 63–69.
[52] T. Nash, Biochem. J. 55 (1953) 416–421.
[53] A. Wolfe, G. Shimer, T. Meehan, Biochemistry 26 (1987) 6392–6396.
[54] M.T. Carter, M. Rodriguez, A.J. Bard, J. Am. Chem. Soc. 111 (1989) 8901–8911.
[55] J.R. Lakowicz, Principles of Fluorescence Spectroscopy, 3rd edn, Plenum Press, New York, 2006.
[56] G. Zhao, H. Lin, S. Zhu, H. Sun, Y. Chen, J. Inorg. Biochem. 70 (1998) 219–226.
[57] D.P. Heller, C.L. Greenstock, Biophys. Chem. 50 (1994) 305–312.
[58] L. Stella, A.L. Capodilupo, M. Bietti, Chem. Commun. (2008) 4744–4746.
[59] Y. Wang, H. Zhang, G. Zhang, W. Tao, S. Tang, J. Luminescence 126 (2007) 211–218.
[60] K. Nakamoto, Infrared and Raman Spectra of Inorganic and Coordination Compounds, Part B: Applications in Coordination, Organometallic and Bioinorganic Chemistry, 6th edn, Wiley, Hoboken, NJ, 2009.
[61] A. Szorcsik, L. Nagy, J. Sletten, G. Szalontai, E. Kamu, T. Fiore, L. Pellerito, E. Kalman, J. Organomet. Chem. 689 (2004) 1145–1154.
[62] A.A. Shamma, H.A. Ali, S. Kamel, Appl. Organomet. Chem. 32 (2017) 3904.
[63] J. Costamagna, F. Caruso, M. Rossi, M. Campos, J. Canales, J. Ramirez, J. Coord. Chem. 54 (2001) 247–259.
[64] R. Smolkova, V. Zelenak, L. Smolko, M. Dusek, Zeit. Kristallogr.-Crystal. Mat. 231 (2016) 715–724.
[65] Y. Wang, N. Okabe, Inorg. Chim. Acta 358 (2005) 3407–3416.
[66] L. Ji, J. Liu, W. Song, Acta Crystallogr. E 67 (2011) 493.
[67] R. Carballo, B. Covelo, E. Garcia-Martinez, E.M. Vazquez-López, Acta Crystallogr. E 57 (2001) 597–599.
[68] Y. Hayashi, S. Santoro, Y. Azuma, F. Himo, T. Ohshima, K. Mashima, J. Am. Chem. Soc. 135 (2013) 6192–6199.
[69] M.A. Uvarova, E.V. Kushan, M.V. Andreev, A.O. Voroshilina, S.E. Nefedov, Russ. J. Inorg. Chem. 57 (2012) 1232–1243.
[70] J. Su, J. Gu, D. Xu, Acta Crystallogr. E 61 (2005) 1033–1035.
[71] Y. Ren, Y. Liu, W. Song, Acta Crystallogr. E 63 (2007) 1191–1193.
[72] N. Xing, L. Xu, F. Bai, H. Shan, Y. Xing, Z. Shi, Inorg. Chim. Acta 409 (2014) 360–366.
[73] S. Caglar, Z. Heren, O. Buyukgungor, J. Coord. Chem. 64 (2011) 1289–1298.
[74] X. Wang, L. Sun, Acta Crystallogr. E 68 (2011) 16.
[75] L. Tabrizi, P. McArdle, M. Ektefan, H. Chiniforoshan, Inorg. Chim. Acta 439 (2016) 138–144.
[76] S. Roy, I. Oyarzabal, J. Vallejo, J. Cano, E. Colacio, A. Bauza, A. Frontera, A. Kirillov, M.G.B. Drew, S. Das, Inorg. Chem. 55 (2016) 8502–8513.
[77] A. Bailey, W.P. Griffith, D.W.C. Leung, A.J.P. White, D.J. Williams, Polyhedron 23 (2004) 2631–2636.
[78] D. Singh, J.B. Baruah, Cryst. Growth Des. 12 (2012) 2109–2121.
[79] L.P. Battaglia, A. Bonamartini-Corradi, G. Marcotrigiano, L. Menabue, G.C. Pellacani, Inorg. Chem. 18 (1979) 148–152.
[80] L. Yang, D.R. Powell, R.P. Houser, Dalton Trans. (2007) 955–964.
[81] A. Okuniewski, D. Rosiak, J. Chojnacki, B. Becker, Polyhedron 90 (2015) 47–57.
[82] X. Chen, B. Ye, X. Huang, Z. Xu, J. Chem. Soc. Dalton Trans. (1996) 3465–3468.
[83] W.D. Horrocks, J.N. Ishley, B. Holmquist, J.S. Thompson, J. Inorg. Biochem. 12 (1980) 131–141.
[84] D. Dobrzynska, T. Lis, J. Wozniak, Acta Crystallogr. E 62 (2006) 1006–1008.
[85] W.D. Horrocks, J.N. Ishley, R.R. Whittle, Inorg. Chem. 21 (1982) 3270–3274.
[86] A.M. Atria, P. Cortes-Cortes, M.T. Garland, R. Baggio, K. Morales, M. Soto, G. Corsini, J. Chil. Chem. Soc. 56 (2011) 786–792.
[87] L.H. Abdel-Rahman, L.P. Battaglia, D. Cauzzi, P. Sgarabotto, M.R. Mahmoud, Polyhedron 15 (1996) 1783–1791.
[88] M. Tas, S. Topal, S. Camur, Z. Yolcu, O. Celik, Main Group Met. Chem. 37 (2014) 39–47.
[89] H. Zhao, F. Yin, X. Xu, L. Han, Acta Crystallogr. E 68 (2012) 533.
[90] R. Cini, G. Giorgi, A. Cinquantini, C. Rossi, M. Sabat, Inorg. Chem. 29 (1990) 5197–5200.
[91] B.M. Zeglis, V.C. Pierre, J.K. Barton, Chem. Commun. (2007) 4565–4579.
[92] Q. Zhang, J. Liu, H. Chao, G. Xue, L. Ji, J. Inorg. Biochem. 83 (2001) 49–55.
[93] A.M. Pyle, J.P. Rehmann, R. Meshoyrer, C.V. Kumar, N.J. Turro, J.K. Barton, J. Am. Chem. Soc. 111 (1989) 3053–3063.
[94] A. Dimitrakopoulou, C. Dendrinou-Samara, A.A. Pantazaki, M. Alexiou, E. Nordlander, D.P. Kessissoglou, J. Inorg. Biochem. 102 (2008) 618–628.
[95] A. Patra, B. Sen, S. Sarkar, A. Pandey, E. Zangrando, P. Chattopadhyay, Polyhedron 51 (2013) 156–163.
[96] J.L. Garcia-Giménez, M. Gonzalez-Alvarez, M. Liu-Gonzalez, B. Macias, J. Borras, G. Alzuet, J. Inorg. Biochem. 103 (2009) 923–934.
[97] W.D. Wilson, L. Ratmeyer, M. Zhao, L. Strekowski, D. Boykin, Biochemistry 32 (1993) 4098–4104.
[98] C. Tan, J. Liu, H. Li, W. Zheng, S. Shi, L. Chen, L. Ji, J. Inorg. Biochem. 102 (2008) 347–358.
[99] V. Rajendiran, R. Karthik, M. Palaniandavar, H. Stoeckli-Evans, V.S. Periasamy, M.A. Akbarsha, B.S. Srinag, H. Krishnamurthy, Inorg. Chem. 46 (2007) 8208–8221.
[100] O.H. Laitinen, V.P. Hytönen, H.R. Nordlund, M.S. Kulomaa, Cell. Mol. Life Sci. 63 (2006) 2992–3017.